



**Citation:** H.-H. Kassemeyer, F. Kluge, E. Bieler, M. Ulrich, J. Grüner, S. Fink, M. Dürrenberger, R. Fuchs (2022) Trunk anatomy of asymptomatic and symptomatic grapevines provides insights into degradation patterns of wood tissues caused by Esca-associated pathogens. *Phytopathologia Mediterranea* 61(3): 451-471. doi: 10.36253/phyto-13154

**Accepted:** October 20, 2022

**Published:** November 25, 2022

**Copyright:** © 2022 H.-H. Kassemeyer, F. Kluge, E. Bieler, M. Ulrich, J. Grüner, S. Fink, M. Dürrenberger, R. Fuchs. This is an open access, peer-reviewed article published by Firenze University Press (<http://www.fupress.com/pm>) and distributed under the terms of the Creative Commons Attribution License, which permits unrestricted use, distribution, and reproduction in any medium, provided the original author and source are credited.

**Data Availability Statement:** All relevant data are within the paper and its Supporting Information files.

**Competing Interests:** The Author(s) declare(s) no conflict of interest.

**Editor:** Luisa Ghelardini, University of Florence, Italy.

**ORCID:**

H-HK: 0000-0001-8675-787X

JG: 0000-0003-1673-5071

RF: 0000-0001-5056-5323

Research Papers

## Trunk anatomy of asymptomatic and symptomatic grapevines provides insights into degradation patterns of wood tissues caused by Esca-associated pathogens

HANNS-HEINZ KASSEMAYER<sup>1,5,\*</sup>, FABIAN KLUGE<sup>1</sup>, EVI BIELER<sup>4</sup>, MARKUS ULRICH<sup>6</sup>, JÖRG GRÜNER<sup>2,3</sup>, SIGFRIED FINK<sup>2</sup>, MARKUS DÜRRENBERGER<sup>4</sup>, RENÉ FUCHS<sup>1</sup>

<sup>1</sup> State Institute for Viticulture and Enology Freiburg, Plant Pathologie & Diagnostics, 79100 Freiburg im Breisgau, Germany

<sup>2</sup> Albert-Ludwigs-Universität Freiburg, Faculty of Environment and Natural Resources, Forest Botany, Albert-Ludwigs-Universität Freiburg, 79085 Freiburg im Breisgau, Germany

<sup>3</sup> FVA - The Forest Research Institute Baden-Wuerttemberg, Forest Protection, 79100 Freiburg im Breisgau, Germany

<sup>4</sup> University Basel, Swiss Nano Science Institute, Nano Imaging Lab, 4056 Basel, Switzerland

<sup>5</sup> Albert-Ludwigs-Universität Freiburg, Faculty of Biology, Plant Biomechanics Group and Botanic Garden, 79104 Freiburg im Breisgau, Germany

<sup>6</sup> Center for Agricultural Technology Augustenberg (LTZ), Plant health & Pesticide reduction, 76227 Karlsruhe, Germany

\*Corresponding author. E-mail: [hanns-heinz.kassemeyer@wbi.bwl.de](mailto:hanns-heinz.kassemeyer@wbi.bwl.de)

**Summary.** Wood colonizing fungi are specialists that exploit the lignocellulose of cell wall components in host wood cylinders as a carbon sources. Some of these specialized fungi, including *Fomitiporia mediterranea* (Fmed) and *Phaeoconiella chlamydospora* (Pch), cause the disease Esca of grapevine. This disease complex includes grapevine leaf stripe disease (GLSD) of canopies and white rot and black wood streaking in trunks. The present study gained insights into the activity of Esca pathogens in host xylem of the trunk tissues at an anatomical level. Lesions with white rot and brown wood streaking were microscopically analyzed, and the structures of affected tissues were compared with intact xylem. In trunks with white rot, demarcation zones separated intact tissues from the lesions. Immediately adjacent to the demarcation zones, cell wall decomposition initiated in the xylem. At this initial stage, cavities appeared in the secondary cell walls of libriform fibres, which expanded and closely resembled the degradation pattern of soft rot. In the advanced stage, the fibre cell walls were completely decomposed, and the vessels were attacked with a degradation pattern similar to white rot. Only remnants of the xylem elements remained, forming amorphous matrices. These decomposition patterns occurred in field samples and in wood cores artificially infected with Fmed. The obvious compartmentalization of the tissue affected by Fmed indicated a defense reaction in the xylem, according to the CODIT model. In contrast, brown wood streaking affected only small groups of vessels, adjacent libriform fibres and parenchyma. Dark inclusions in cells and tyloses in vessels indicate a defense reaction against the pathogens

causing brown wood streaking. Artificial inoculation of sterile wood cores with Pch confirmed the contribution of this pathogen to brown wood streaking. This research provides insights into the structural and functional anatomy of intact and infected tissues of grapevines, which clarify the etiology of Esca, and provide new knowledge for developing new approaches to control of this disease complex.

**Keywords.** White rot, xylem, cell wall degradation, CODIT-model, *Fomitiporia mediterranea*, *Phaeoconiella chlamydospora*.

## INTRODUCTION

Grapevines (*Vitis vinifera*) are woody liana plants, with anatomical structure of the secondary xylem adapted to the climbing vine growth habit. The secondary xylem of woody plants is a niche for specialist fungi that can exploit cell wall lignocellulose as carbon sources as well as ions dissolved in the hydrosystem (Yadeta and Thomma 2013). Secondary xylem of grapevine provides substrates for several wood-colonizing fungi causing grapevine trunk diseases (GTDs), including Esca. Esca has been known for many years (Viala 1926; Mugnai et al., 1999), but in the last three decades, the increasing incidence of this disease has gained economic importance as it causes premature vine decline. (Gramaje et al., 2018; Guerin-Dubrana et al., 2019).

Grapevine leaf stripe disease (GLSD) is the most obvious and distinct manifestation of Esca, but GLSD was designated by Surico (2009) as a particular disease complex. There is a consensus that Esca, including GLSD, is caused by colonization of host secondary xylem by wood-destroying fungi. In xylem of affected trunks zones develop with characteristic symptoms of white rot and brown streaking (Viala, 1926; Mugnai et al., 1999; Chiarappa, 2000; Surico et al., 2000; Surico 2009; Bertsch et al., 2013; Bruez et al., 2016; 2020; Gramaje et al., 2018; Mondello et al., 2018; Fischer and Peighami Ashnaei, 2019; Hrycan et al., 2020; Vaz et al., 2020; Pacetti et al., 2021).

White rot in grapevine trunks is caused by species of *Basidiomycota*, including *Fomitiporia mediterranea* (Larignon and Dubos 1997; Mugnai et al., 1999; Cortesi et al., 2000; Fischer, 2001; Fischer and Kassemeyer, 2003; Larsson et al., 2006; Hofstetter et al., 2012; Bertsch et al., 2013; Bruez et al., 2016; 2020; Baranek et al., 2018; Elena et al., 2018; Del Frari et al., 2019; 2021; Brown et al., 2020; Moretti et al., 2021; Ye et al., 2021; Pacetti et al., 2022). Other species of the *Hymenochaetales* are also involved, including *Tropicoporus* sp., *Inonotus* sp., *Fomitoporella* sp. and *Phellinus* sp. (Cloete et al., 2015; Brown et al., 2020). Two types of white rot of woody plants have been described: (i) selective delignification, where first lignin and then hemicellulose and cellulose are preferentially degrad-

ed; and (ii) simultaneous degradation of all cell wall components (Blanchette, 1984; Schwarze, 2007). The causal agents of brown wood streaking include *Ascomycota* species from *Phaeoconiellales* (e.g. *Phaeoconiella chlamydospora* and *Phaeoacremonium minimum* (teleomorph *Togninia minima*)), and *Botryosphaeriales* (e.g. *Diplodia seriata* and *Neofusicoccum parvum*) (Larignon and Dubos 1997; Crous and Gams 2000; Crous et al., 2006; Úrbez-Torres et al., 2008; 2011; Mutawila et al., 2011; Lecomte et al., 2012; Fischer et al., 2016; Massonnet et al., 2017; 2018a; b; Reis et al., 2019; Claverie et al., 2020).

Restricted areas of brown wood streaking are most likely the result of host defense reactions such as deposition of phenolic compounds in the affected cells (Troccoli et al., 2001; Del Rio et al., 2004; Bruno and Sparapano, 2006b, 2007; Agrelli et al., 2009; Amalfitano et al. 2011; Mutawila et al., 2011; Lambert et al., 2012, 2013; 2012; Calzarano et al., 2016; Gómez et al., 2016; Pierron et al., 2016; Rusjan et al., 2017; Spagnolo et al., 2017; Stempien et al., 2017; Khattab et al., 2020; Labois et al., 2020, 2021). The numerous studies on the pathogen spectrum of Esca (including GLSD) and on the host plant responses have provided valuable insights into the etiology of the disease. However, detailed knowledge is not available on the degradation patterns caused by these pathogens in xylem of affected grapevines.

The present study aimed to gain insights into the decomposition patterns in grapevine secondary xylem, caused by two Esca pathogens. The architecture of secondary xylem plays a crucial role in the colonization dynamics by the pathogens. For this reason, visualization of the structural and functional anatomy of this host tissue was required. Based on anatomical knowledge, a detailed characterization became possible of the degradation patterns in the secondary xylem of infected trunks. Wood samples from trunks of symptomatic and asymptomatic grapevines, and from wood cores artificially inoculated with *Fomitiporia mediterranea* (Fmed) and *Phaeoconiella chlamydospora* (Pch), were examined using microscopy. Pathogen pathways in trunk tissues and the decomposition processes caused by the fungi were characterized.

## MATERIAL AND METHODS

### *Sampling and macroscopic documentation*

In 2019, 2020 and 2021, trunks of *Vitis vinifera* L. “Mueller-Thurgau” and “Pinot noire” vines expressing GLSD symptoms were collected from experimental plots at the State Institute for Viticulture in Freiburg (Germany). Samples of asymptomatic grapevines from the same experimental plots were used for comparisons. The grapevines were planted in 1999 (“Mueller-Thurgau”) and 1983 (“Pinot noire”), and were in adjacent plots on loess-clay soil facing southwest, located south of Freiburg (Germany) (47°45'20"N; 7°50'04"E; 280 m altitude). Incidence of Esca was 46.2% for the “Mueller-Thurgau” vines and 27.0% for “Pinot noir”. In addition, samples from 2003 were collected from the same field, and further samples were collected between 2014 and 2018 from GLSD-symptomatic and asymptomatic grapevines from different regions of southwestern Germany. Longitudinal and cross-sections were made from the trunks with a band saw and the conditions of the sections were documented. For the microscope analyses, samples each measuring 10 × 8 × 4 mm were excised from wood segments with lesions and intact secondary xylem. Furthermore, approx. 1 cm thick transverse or longitudinal sections of trunks were rubbed with sandpaper of increasing grit size (80 to 480) to produce surfaces for stereo microscope observation.

### *Artificial inoculation of wood cores*

From GLSD-asymptomatic grapevines grown in the vineyard described above, cores of 5 mm diameter were taken from the central areas of sampled trunks using a drill bit (5 mm diam.). Trunk sampling was radial, that all zones of each wood cylinder were included in the drill core. The wood cores were then autoclaved (121°C, 20 min.) to avoid contamination by pathogenic and endophytic fungi. The samples were then placed into Petri dishes (90 mm diam.) containing malt extract agar (30 g malt extract, 5 g yeast extract, 20 g agar, 1 L deionized water), and were inoculated with mycelium pieces from *Fomitiporia mediterranea* M. Fischer, (accession No. 45/23 from *V. vinifera* cv. Mueller-Thurgau Blankenhornsberg) or *Phaeoconiella chlamydospora* Gams W., Crous P., Wingfield M.J & Mugnai L., (accession No. CBS 229.95), and were incubated at 24°C. Samples were taken from the inoculated wood cores 2 to 4 months after inoculation for the preparation of semi-thin wood sections.

### *Light microscopy*

The wood specimens were fixed in 2% glutardialdehyde in phosphate buffer (pH 7.4) in a vacuum for 24 h and then rinsed three times in deionized water. The samples were then dehydrated in an increasing concentration of isopropanol, and then embedded in methacrylate resin. Semi-thin sections (3 µm and 1 µm) were made with a rotation microtomes (LEICA Reichert & Jung Supercut 2065 and 2044). The sections were rinsed overnight in isopropanol to remove the resin, and were then fixed on glass slides and stained in a programmable slide stainer (ZEISS HMS TM Series) with 2 % safranin and 1% acriflavine (12 h), 1% acid-yellow (30 min) and 1% methylene-blue (5 min). For fluorescence microscopy (FM), the slides were stained with 5 µM acridine orange. After staining, the specimens were embedded in Eukitt (O. Kindler). The microscopic analyses were carried out with a light (brightfield) and fluorescence microscope (ZEISS Axio Imager Z1, Carl Zeiss AG), equipped with the optical sectioning system (ZEISS Apotome 2) for structural illumination and a digital imaging system (ZEISS Axiocam MR35, ZEN 2,9 pro imaging processing software, Carl Zeiss AG). The specimens stained with acridine orange were analysed by epifluorescence using the FITC filter combination 38 HE (excitation 460-488 nm, emission 500-557 nm). The overview images of the wood longitudinal and cross sections were acquired using a ZEISS Stereo LumarV12 with motorized x-, y-, z-axis positioning control, and ZEISS Axiocam 305 and ZEN 3.2 pro image processing software (Carl Zeiss AG).

### *Scanning electron microscopy*

Host xylem structure was visualized using a scanning electron microscope (SEM). The surfaces of specimens excised as described above were ground and polished using the Leica EM TXP Target Surfacing System (Leica Microsystems) before being examined in the SEM. After sputtering the specimens with 20 nm of gold, the wood structure was analyzed using a High Resolution Field-Emission (Cold Emission) Scanning Microscope FEI Nova Nano SEM 230 (FEI Company). To preserve the structure of the fungi colonizing the wood tissues, fresh samples were additionally analyzed with a Cryo-SEM (Philips XL30 ESEM, Koninklijke Philips N.V.) equipped with a cryo preparation unit (Gatan Alto 2500, Gatan Inc.). Small slices (approx. 4 mm thick) were excised from trunk segments with a scalpel, and were mounted on specimen holders with low-temperature mounting medium. Cryofixation was carried out using

nitrogen slush ( $< -185^{\circ}\text{C}$ ) in the cryo-preparation unit. The frozen samples were then sputtered with 20 nm gold in a high vacuum cryo-preparation chamber, and examined with a SE detector operating with an acceleration voltage of 5–10 kV at high vacuum and  $-150^{\circ}\text{C}$ . The SEM and Cryo-SEM images were acquired and documented with DISS5 Software from REM-X GmbH Bruchsal.

## RESULTS

### *Anatomy of intact host secondary xylem*

In the cross-sections of both varieties, wide-lumened vessels occurred more frequently in the early wood than in the late wood, followed by a number of narrow-lumened vessels (Figure 1, Figure 2 A and B). The lateral walls of the vessels and tracheids were scalariform with bordered pits (Figure 3 A and B; Figure 4 A). In the centre of the pits, the middle lamella and primary cell wall formed a membrane (Figure 3 A). A paratracheal sheath of parenchymatic cells was associated with each vessel, which extended parallel in axial direction (Figure 2 A; Figure 4 A). Semi-bordered pits connected the vessels with the associated cells (vessel associated cells - VACs) of the paratracheal sheaths (Figure 4 A). Longitudinal and tangential sections showed that each vessel formed an axial continuum without transverse walls over a long distance due to the remission of the transverse walls (Figure 4 B). In contrast, the tracheids had compartments whose lateral walls tapered at the apex and formed an end plate (Figure 4 B). A row of thick-walled,

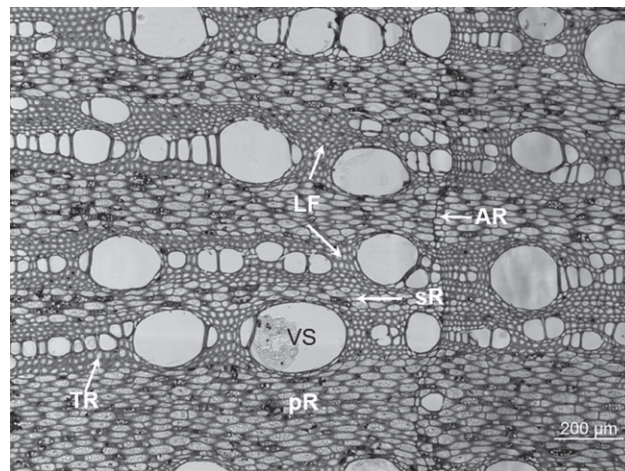


**Figure 1.** Cross section from intact xylem of *Vitis vinifera* “Mueller-Thurgau”. Xylem with vessels (VS), tracheids (TR), libriform fibres (LF) primary wood rays (pR), secondary wood ray (sR), and annual ring (AR) are indicated. Bright field micrograph, 5× magnification.

libriform fibres surrounded the vessels and tracheids, forming a compact bond without intercellular spaces (Figure 5). Radial and tangential sections displayed tapered longitudinal tips of the libriform fibres, similar to the tracheids (Figure 4 B). Fluorescence microscopy revealed the highly fluorescent middle lamella and the different layers of libriform fibre cell wall (cw) in the samples stained with acridine orange. A thick laminated structure ( $S_2$  layer) was visible between a thin outer (primary cell wall and  $S_1$  layer of secondary cell wall) and inner  $S_3$  layer (Figure 5). Pits, each containing a septum

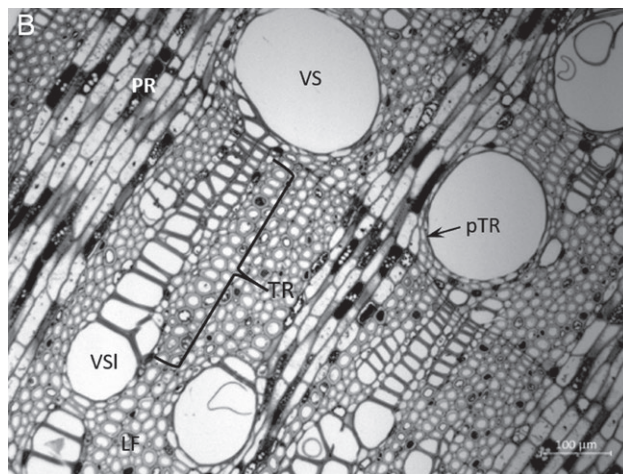
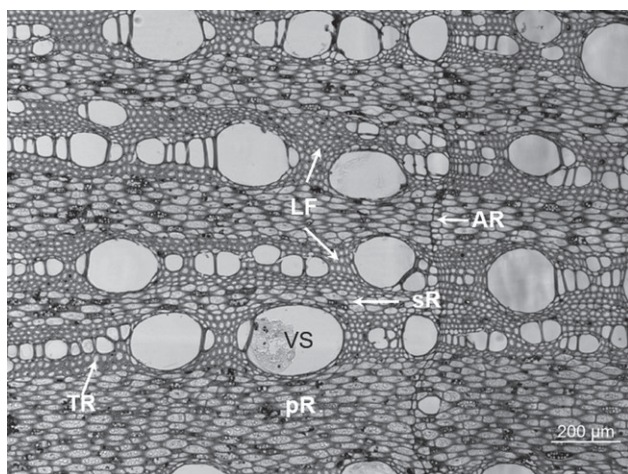


**Figure 2.** Cross section of intact xylem of *Vitis vinifera* “Mueller-Thurgau”. (A) Detail of a wide lumen vessel (VS), paratracheal parenchyma (pTR), tracheids (TR), libriform fibres (LF), parenchyma of a primary wood ray (PR), and parenchyma cells filled with starch grains (ST). Brightfield micrograph, 10× magnification. (B) Series of tracheids within a single annular ring. Wide lumen early wood vessel (VS), and a late wood vessel (VSI). Bright field micrograph, 10× magnification.

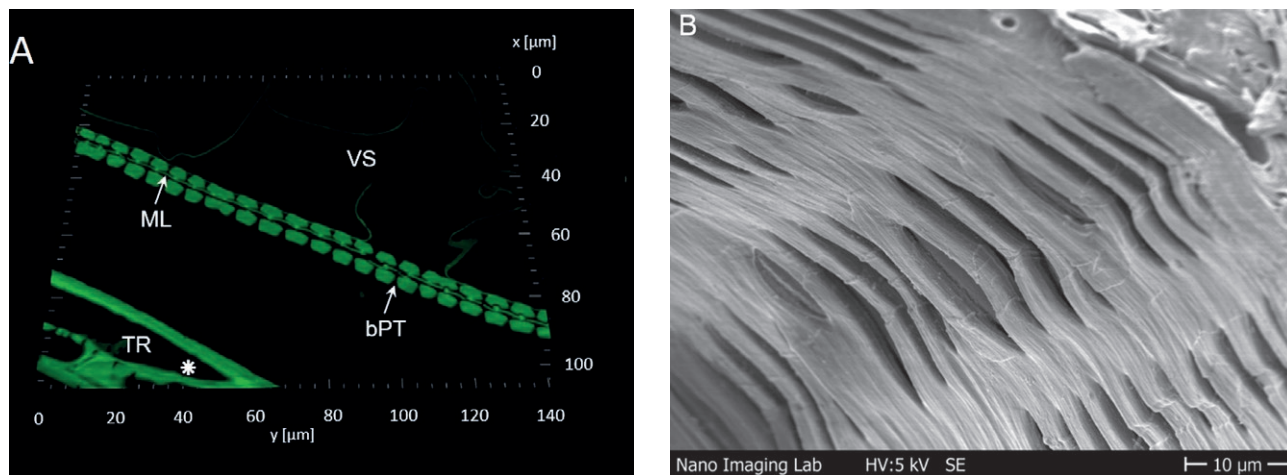


**Figure 3.** Cross section of asymptomatic xylem of *Vitis vinifera* “Pinot Noir”. (A) Scalariform lateral cell wall between tracheids and vessels is formed by bordered pits (bPT). The middle lamella (ML) forms the pit membrane, and a tracheid (TR) with endplate (\*) are indicated. Fluorescence microscopy 3D image, excitation (460–488 nm, emission 500–557 nm). 63× magnification. (B) Vessel with scalariform pitting at the lateral wall. Scanning electron micrograph, 2000× magnification.

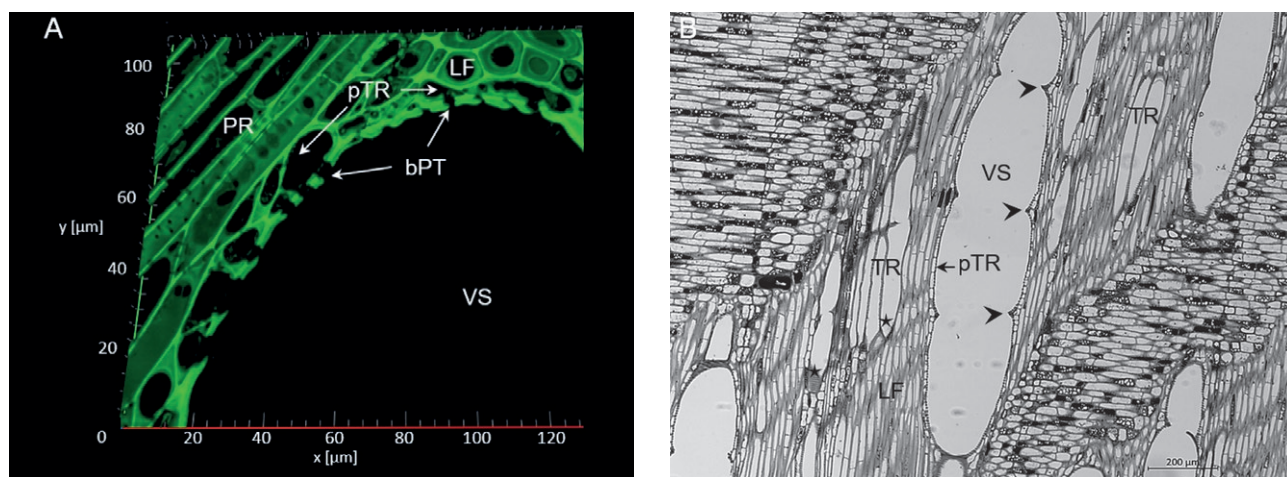


**Figure 4.** Tracheids (TR) and vessel (VS) from asymptomatic xylem of *Vitis vinifera* “Mueller-Thurgau”, longitudinal section. (A) Wide lumen vessel (VS) with semi-bordered pits (bPT), vessels surrounded by a sheath of paratracheal parenchyma (pTR), libriform fibres (LF), and a wood ray (PR) are indicated. Fluorescence microscopy 3D image, 63× magnification. (B) Vessel (VS) with remitted cross walls (arrow heads), tracheids with endplate (★), and paratracheal sheet of parenchyma (pTR). Bright field micrograph, 5× magnification.

composed of the middle lamella, connected the lumina of the libriform fibres to each other and to the adjacent parenchyma cells (Figure 5). The primary and secondary wood rays consisted of elongated parenchymatous cells filled with starch grains (Figures 1; 2 A and B; 4 A; 5).

*Trunks with GLSD had different types of lesions in the wood cylinders*

In vines with characteristic GLSD canopy symptoms, macroscopically visible necrotic lesions were always evident in longitudinal and cross sections of

the trunks. However, plants with GLSD-symptomless canopies also had these lesions. Two different patterns occurred in the trunks: (i) extended lesions with white rot, and (ii) dark brown to black spots in radial sections and streaks in longitudinal sections.

White rot was clearly visible as pale brown zones each with a central ochre amorphous mass (Figure 6). In cross section, black demarcation lines clearly separated the lesions from apparently intact wood (Figures 6; 8 A and B). The lines were more or less concentric, but often showed protuberances with second or third lines, forming distinct compartments (Figure 6). In longitudinal

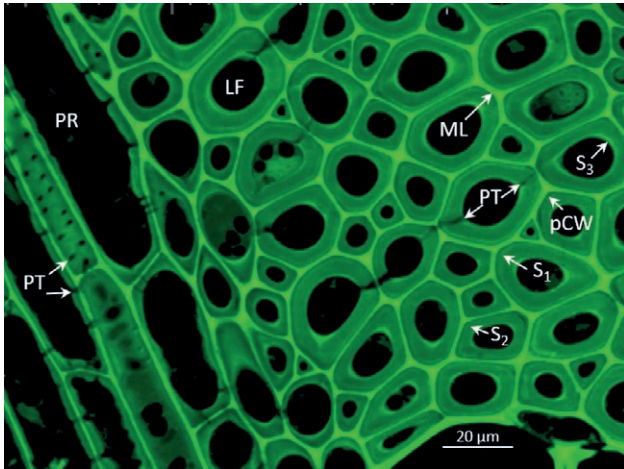


**Figure 5.** Cross section of libriform fibres (LF) from asymptomatic xylem of *Vitis vinifera* “Mueller-Thurgau”. Middle lamella (ML) filling the cell corners, and the primary cell wall (pCW) are indicated. The laminated secondary cell wall, and the exterior  $S_1$ - and the innermost  $S_3$ -layer enclose the central thick  $S_2$ -layer. Pits (PT) connecting fibre cells and parenchyma cells (PR) are also indicated. Fluorescence micrograph 63 $\times$ , excitation 460-488 nm, emission 500-557 nm.

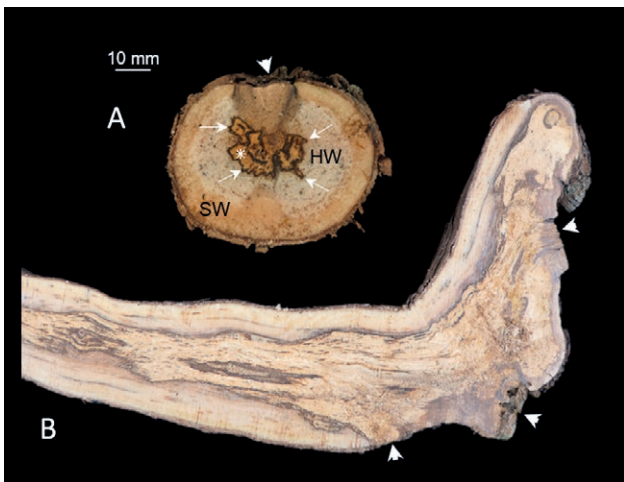


**Figure 6.** Cross section of a symptomatic (GLSD) xylem of *Vitis vinifera* “Pinot noir” and longitudinal section of a symptomatic (GLSD) *Vitis vinifera* “Mueller-Thurgau” trunk. Xylem with white rot lesions extending from wounds (arrow heads) into the trunk center, protuberances of the demarcation lines (arrows) are clearly visible; in some parts the pathogen has passed the primary demarcation line and colonized further areas of the xylem causing a compartmentalization of the white rot by secondary demarcation lines (\*), sapwood (SW), heartwood (HW). Bright field micrograph 0.8 $\times$ .

sections, the lesions spread from the top of the trunks to the bases, thinning downwards (Figure 6). The white rot originated from pruning wounds, and from there penetrated into the middle of the trunks (Figure 6).

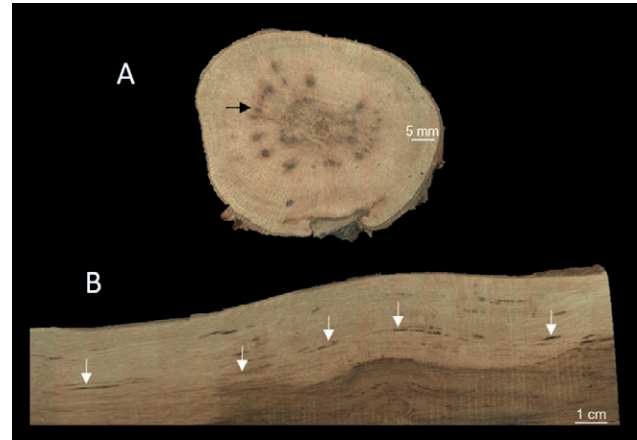


**Figure 7.** Trunk of a symptomatic (GLSD) *Vitis vinifera* “Mueller-Thurgau”. Cross section with a concentric ring of black spots (black arrow); longitudinal section traversed by black streaks visible as a discontinuous line due to the torsional growth (white arrows). Bright field micrograph 0.8 $\times$ .

In addition, dark brown to black spots were evident in the trunk cross-sections, often arranged in concentric groups or rings. (Figure 7). In longitudinal sections, these spots were as more or less short, dark streaks. However, if an imaginary line was drawn along the dark streaks, they each traversed the trunk in a continuous row for a considerable distance in the longitudinal direction (Figure 7).

#### *Xylem elements naturally affected by white rot had specific decomposition patterns*

Light microscopy and SEM visualized the structures of the host tissues and cells in the lesions affected by white rot. In each demarcation zone, the parenchymatic cells and the libriform fibres contained dark inclusions, and the vessels were obstructed by tyloses (Figure 8 A and B). Adjacent to the demarcation line, round cavities were seen in the  $S_2$  layer of each fibre cell wall (Figure 9 A). The pits in the cell walls were frequently dilated and widened toward the unaffected middle lamella (Figure 9 A). These cavities enlarged the closer the cells were to the lesion centres, often became tubular (Figure 9 B). At advanced stages, the entire  $S_2$  layers were decomposed and only the middle lamella and primary cell walls, as well as the  $S_3$  layers, remained (Figure 9 B). In the vessels, vascular tracheids and wood rays resisted degradation until a late stage of decay (Figure 9 C). Observations with Cryo-SEM showed that fungi were evident in affected vessels, in which branched hyphae formed mycelia (Figure 10 A). In the central parts of lesions, a

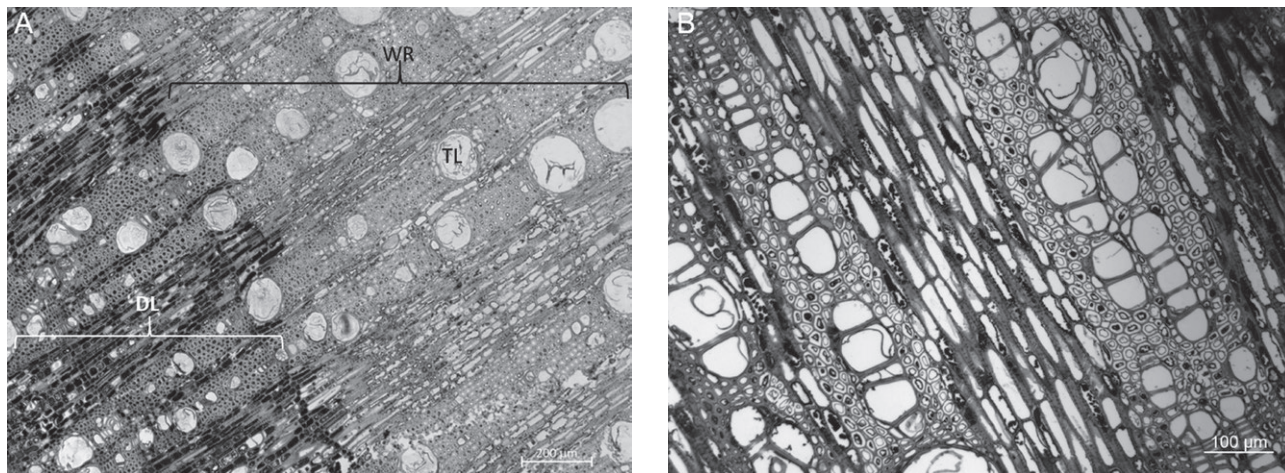


**Figure 8.** Cross section of the affected by white rot like lesions. (A) Demarcation zone (DL) with darker coloration of xylem elements, inwards with rot like lesion (WR), vessels with tylosis (TL). Bright field 5x. (B) Overview of a white rot like lesion, with decomposed  $S_2$ -layer of libriform fibers, the lumen of vessels is filled with tylosis and the parenchyma cells show dark inclusions. Bright field micrograph 10x.

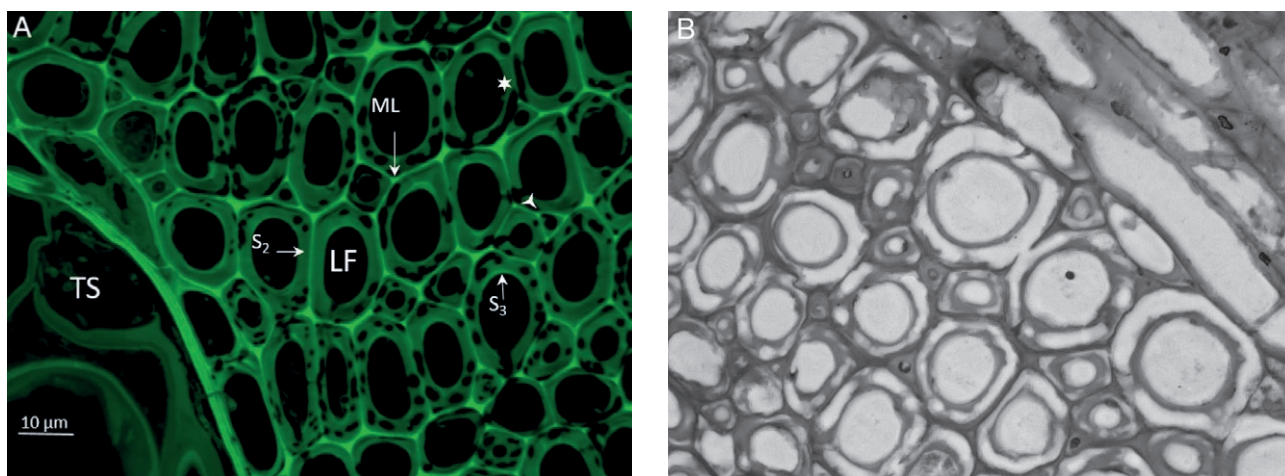


**Figure 9.** Cross section of the affected by white rot like lesions. (A) Initial decay with round caverns in the  $S_2$ -layer ( $S_2$ ) of libriform fibres (LF), middle lamellae with primary cell wall and adjacent  $S_1$ -layer (ML) as well as  $S_3$ -layer ( $S_3$ ) are the still intact, vessel filled by tylosis (TS), in advanced stages cavities became tubular shaped (★) and pits dilated (▲). Fluorescence micrograph 63x, excitation 460–488 nm, emission 500–557 nm. (B) Advanced decomposition of the libriform fibres, the  $S_2$  layer is decomposed, middle lamella, primary cell and  $S_1$  as well  $S_3$ -layer are remaining. Bright field micrograph 63x. (C) White rot like lesions with advanced decay of xylem in the right part of the image, while the libriform fibres are completely degraded, the structures of vessels and tracheids filled by tylosis are still visible. Scanning electron micrograph 100x.



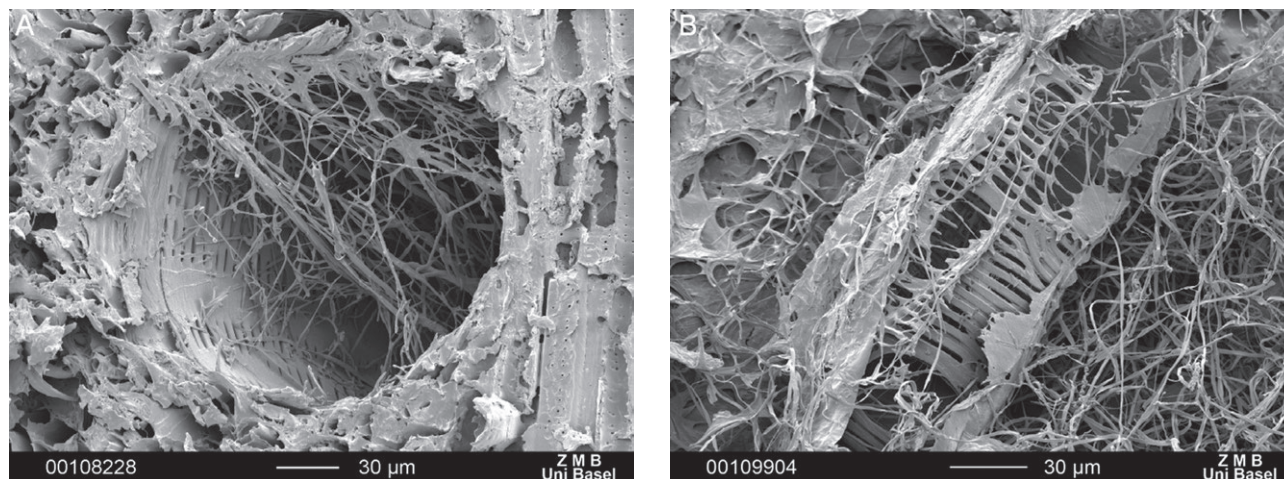


**Figure 10.** Cross-section of a white rot like lesion, *Vitis vinifera* “Mueller-Thurgau”. (A) Vessel with hyphae; Cryo scanning electron micrograph 400 $\times$ . (B) Mycelium with remains of a vessel. Cryo scanning electron micrograph 500 $\times$ .

progressive decay of the secondary xylem proceeded, which finally also affected vessels, vascular tracheids and parenchyma. In this final process, a dense mycelium proliferated over the remains of the tissue, and only an amorphous mass remained, from which isolated remnants of the cell walls were recognizable (Figure 10 B). The decomposition patterns of white rot were the same for both *V. vinifera* cultivars.

#### *Brown spots and streaks of naturally infected trunks displayed different decay patterns*

In cross-section, the brown spots each consisted of individual groups of vessels with the surrounding tissue located between the wood rays within a growth ring. (Figures 7; 11 A). Examination at higher resolution showed that small spots were also scattered over the entire cross-sections in the secondary xylem, encompassing only one small group of vessels (Figure 11 A and D). Semi-thin sections visualized deposits in the lumina of libriform fibres and parenchyma cells, which caused the dark spots and streaks (Figure 11 A, B and C). In these areas, the vessels were obstructed by tyloses, originating from the VACs and invading through the half-bordered pits of the scalariform cell walls (Supplementary Figure 1). The libriform fibres were partially compressed, and high magnification revealed elongated or crescent-shaped cavities in the cell walls (Figure 12 A and B). In this case, the pits were dilated and often funnel-shaped opened towards the cell lumen (Figure 12 A). Weakly branched hyphae sporadically colonized the vessels and parenchymatic cells of the wood rays (Figure 13 A and B).

#### *Artificial inoculation with *Fomitiporia mediterranea* and *Phaeomoniella chlamydospora* resulted in comparable lesion patterns as in the field*

Within 4 d post inoculation (dpi), Fmed had colonized the plant sample surfaces, and 16 dpi ochre-coloured mycelium completely covered the specimen cores. At this stage, fine hyphae permeated the S<sub>2</sub> layers of fibres, which could be distinguished from the pits by their sinuous structure (Figure 14 A). Two months after inoculation, Fmed grew within the cell walls of the libriform fibres and decomposed the S<sub>2</sub> layers, forming round caverns in an identical pattern as seen in the cross sections of samples taken from the field (Figure 14 B). In tangential section, caverns were aligned in a helical pattern at an angle of 50° to 60° in the cell walls of the libriform fibres (Figure 14 C). This alignment was also observed in cross sections when examining round cavities in cell walls at different focal planes (Supplementary Figure 2 Video). Four months after inoculation, advanced decomposition of the S<sub>2</sub> layers occurred (Supplementary Figures 3 A, B, C). In general, the pattern of cell wall decomposition of libriform fibres observed in this study was consistent with that found in white rot lesions of trunks sampled from the field.

In cores inoculated with Pch, isolated hyphae occurred in the secondary xylem two months after inoculation (Figure 15 A). In tangential and cross sections, falciform caverns occurred in each S<sub>2</sub> layer near the middle lamella, and these were similar to those in samples from the field (Figure 15 A; Supplementary Figure 4). In contrast to the cores from plants inoculated with Fmed, the wood inoculated with Pch was only slightly decom-

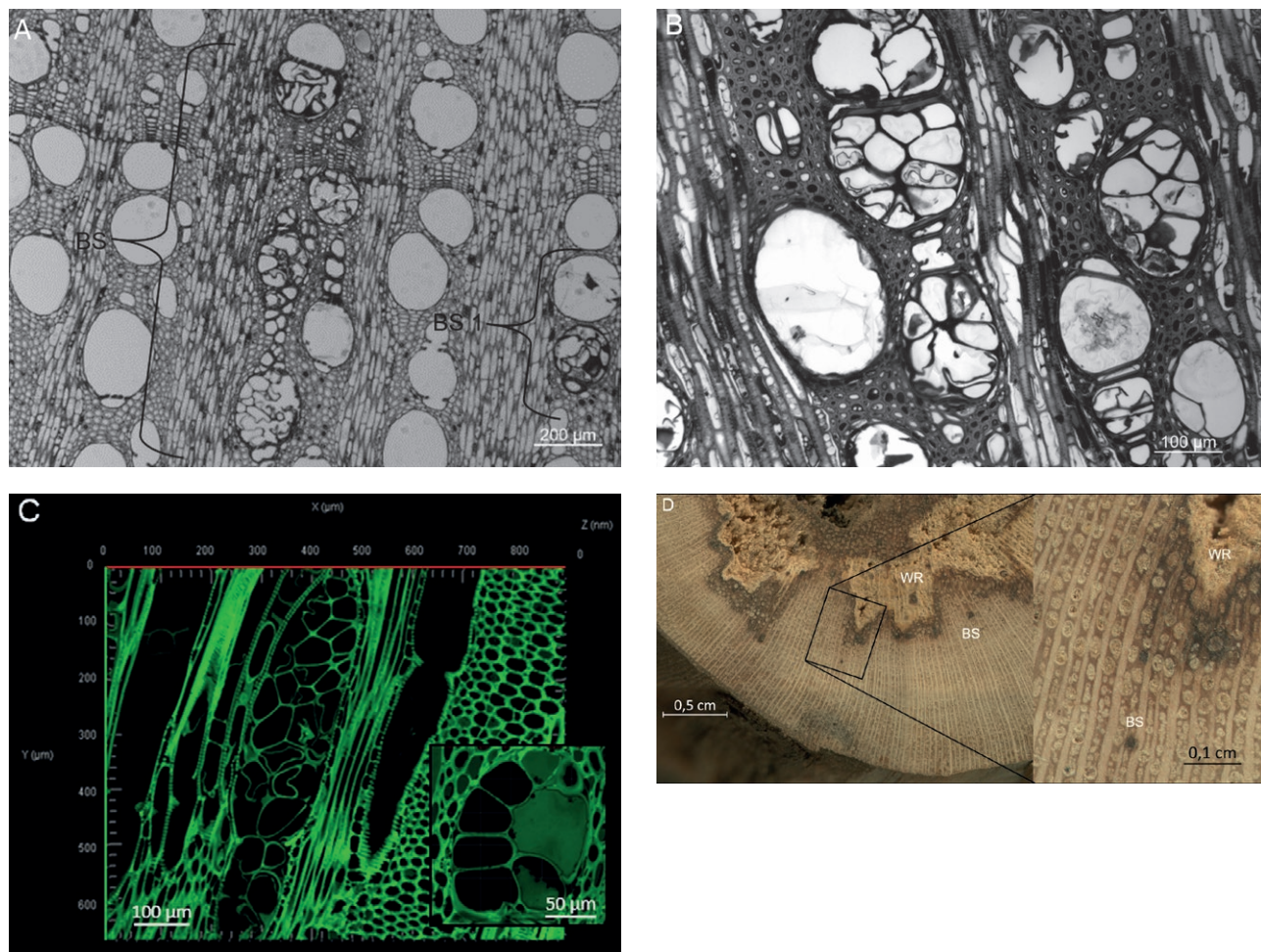


**Figure 11.** Cross section of black spot, *Vitis vinifera* “Mueller-Thurgau”. (A) Wood cylinder, overview with black spots comprising a couple of vascular bundles (BS) and a single vessel interspersed in intact xylem (BS 1); bright field Plan-Neofluar 5×. (B) Vessels obstructed by tylosis in black spots, libriform fibres and parenchyma filled with dark inclusions and slightly deformed. Bright field micrograph 10×. Insert: Cross section of a vessel in a black spot obstructed with tylosis; 3D Fluorescence micrograph 25×. (D) Trunk of a symptomatic *Vitis vinifera* “Mueller-Thurgau”, cross section with a small spot encompassing one vessel, whit rot (WR) in the center. Bright field micrograph 0.8×, display window Bright field micrograph 0.8×.

posed, although mycelium had spread on the wood core surfaces, and hyphae had invaded the vessels (Figure 15 B). As in the naturally infected samples, dark deposits filled the libriform fibres and parenchyma cells, and tylosis obstructed the vessels (Supplementary Figure 5).

### DISCUSSION

The wide lumen vessels and vascular tracheids of the two grapevine varieties exhibited characteristics of a ring-porous xylem, as described by Carlquist (1985; 2010) and Vazquez-Cooz and Mayer (2004). Vessels and tracheids formed axial continua from top to bottom,

which provides high conductivity of plant hydrosystems (Bortolami *et al.*, 2021). Plant vessels can reach lengths of several meters in early wood (Hacke and Sperry, 2001). Measurements of vessel length for *Vitis labrusca* by Zimmermann and Jeje (1981) showed a minimum length of 1 m in >70% of samples. The structure of the vessels found in both cultivars in the present study indicates that long open vessel sections also occur in *V. vinifera*. Pronounced primary and secondary wood rays with parenchyma (RP) cells radially traversed the secondary xylem, as is typical of lianas. (Carlquist 1985, 2010; Gallenmüller *et al.*, 2001; Rowe and Speck, 2004; Masselter and Speck, 2008; Angyalossy *et al.*, 2012). In addition, axial strands of vessel associated parenchy-

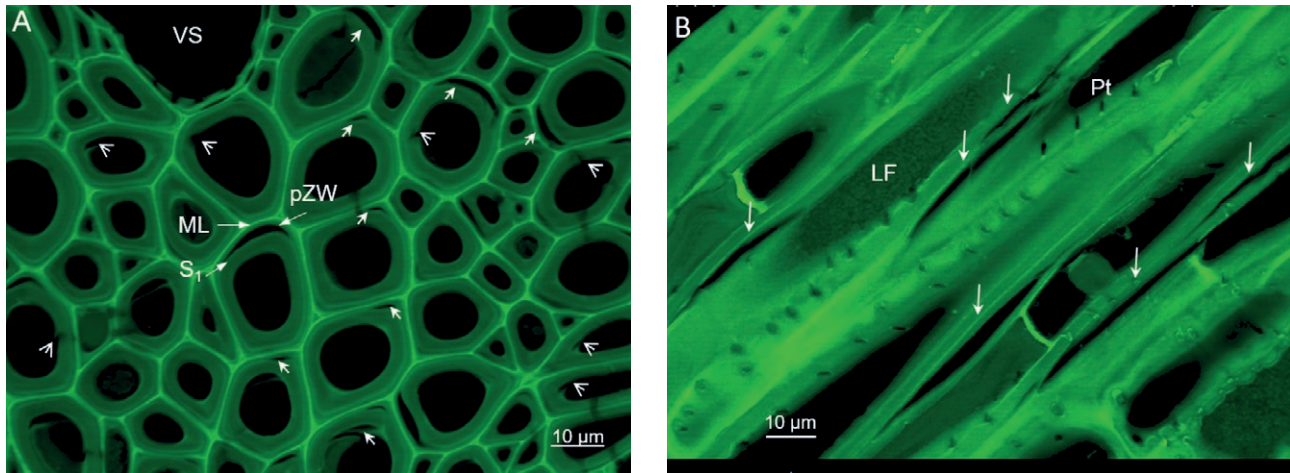


**Figure 12.** Libriform fibres (LF) in black spots and streaks of *Vitis vinifera* “Mueller-Thurgau”. (A) Cross section of libriform fibres with falciform detachments (arrows) of the primary cell wall (pZW) from the  $S_1$ -layer and dilated pits (arrow heads), middle lamella (ML) is intact. Fluorescence micrograph 63 $\times$ , excitation 460–488 nm, emission 500–557 nm. (B) Longitudinal section of libriform fibres, falciform cell wall detachments in axial direction, pits (Pt) interconnect the fibres. Fluorescence micrograph 63 $\times$ , excitation 460–488 nm, emission 500–557 nm.

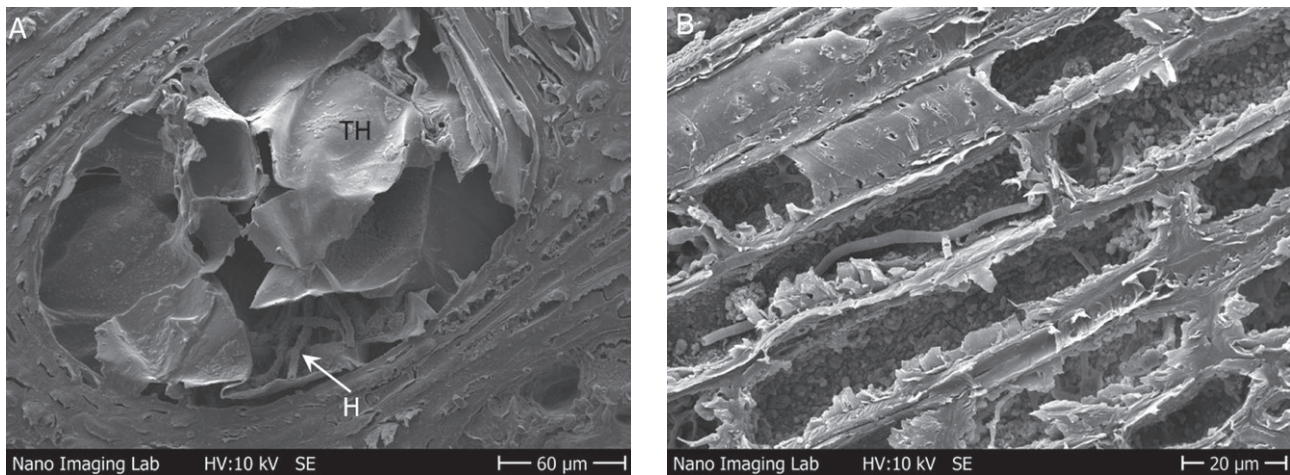


**Figure 13.** Details of black spots and streaks on *Vitis vinifera* “Mueller-Thurgau”; (A) cross-section, vessel with hyphae (H) and tylosis (TH). Cryo scanning electron micrograph 400 $\times$ ; B longitudinal section, parenchyma cells of the wood ray with hyphae. Cryo scanning electron micrograph 1000 $\times$ .

ma cells (VACs) formed paratracheal sheaths of living cells, as described in woody plants by Carlquist (2010) and Morris *et al.* (2016 a; b; 2018). The parenchyma cells of RP and VACs fulfill important functions in secondary xylem, including: (i) sink and source for assimilates, mainly starch, remobilized in spring; (ii) regeneration into secondary cambium to heal injuries; (iii) refilling vessels; (iv) bidirectional transport of water, ions and organic molecules between the symplastic and the apoplastic elements of the secondary xylem; and (v) defense response after infections by pathogens (Carlquist, 2012; Holbrook and Zwieniecki, 1999; Pfautsch *et al.*, 2015 a;

b; Morris *et al.*, 2016 a; b; Morris and Jansen 2016; Morris *et al.*, 2018; Secchi *et al.*, 2017). Numerous pits interconnect secondary xylem elements and ensure exchange and communication between the living cells of RP and VACs and the apoplastic vessels, tracheids and libriform fibres. Of particular importance are the bordered pits at the lateral scalariform wall of vessels and tracheids and the half-bordered pits at the boundaries with RP and VACs. They form an interface between apoplastic xylem elements and the symplast, constituting a three-dimensional network in the plant trunk that extend to the shoot tips (Kedrov, 2013; Sano *et al.*, 2013; Donaldson *et*

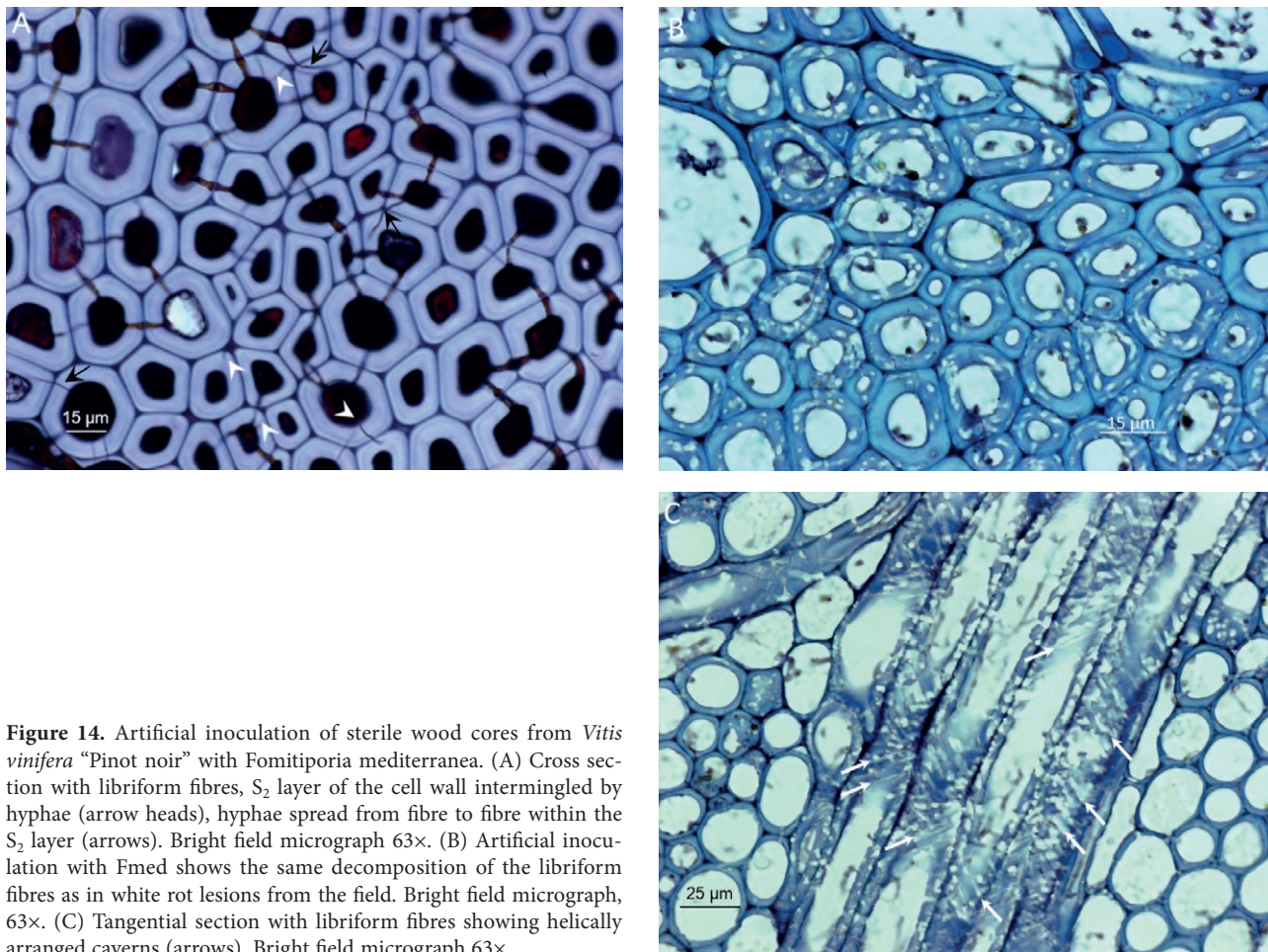


**Figure 14.** Artificial inoculation of sterile wood cores from *Vitis vinifera* “Pinot noir” with *Fomitiporia mediterranea*. (A) Cross section with libriform fibres, S<sub>2</sub> layer of the cell wall intermingled by hyphae (arrow heads), hyphae spread from fibre to fibre within the S<sub>2</sub> layer (arrows). Bright field micrograph 63×. (B) Artificial inoculation with Fmed shows the same decomposition of the libriform fibres as in white rot lesions from the field. Bright field micrograph, 63×. (C) Tangential section with libriform fibres showing helically arranged caverns (arrows). Bright field micrograph 63×.

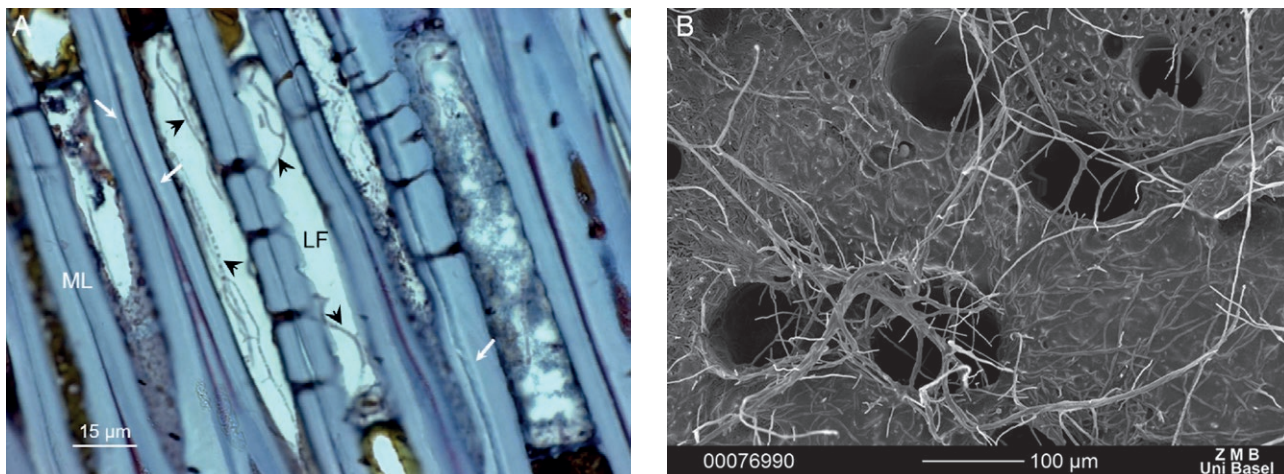


**Figure 15.** Artificial inoculation of sterile wood cores from *Vitis vinifera* “Pinot noir” with *Phaeomoniella chlamydospora*. (A) Libriform fibres (LF), longitudinal section, growing hypha (arrowheads) in axial direction, beginning detachment of the S<sub>2</sub> layer from the middle lamella (ML) and outer cell wall (arrows), Bright field micrograph 63×. (B) Surface of an inoculated core colonized by Pch, hyphae entering the vessels. Scanning electron micrograph 100×.

*al.*, 2018; Morris *et al.*; 2018; Gao *et al.*, 2020; Zhang *et al.*, 2020; Kaack *et al.*, 2021; Koddenberg *et al.*, 2021;).

Structural and functional studies have shown that the vascular architecture of grapevine trunks facilitates dissemination of wood-colonizing pathogens. The wide lumened vessels provide highways for wood-colonizing pathogens to pass axially through trunks (Pouzoulet *et al.*, 2014, 2017, 2020; Bruez *et al.*, 2020). Longitudinal sections through trunks verified the large-scale colonization of secondary xylem and confirmed that wounds are entry ports for wood-degrading pathogens (Rolshausen *et al.*, 2010; Travadon *et al.*, 2013; 2016; Claverie *et al.*, 2020; Martinez-Diz *et al.*, 2020). In addition, the scalariform cell walls facilitate the passage of pathogen hyphae from vessels into adjacent libriform fibres, where the hyphae proliferate laterally via the numerous pits.

The extensive lesions observed in the secondary xylem macroscopically resembled typical white rot of woody plants (Blanchette 1984; Schwarze, 2007; Goodell *et al.*, 2008; Daniel *et al.*, 2004; 2014; Hastrup *et al.*, 2012). However, greater magnification revealed decomposition patterns in the affected zones of the secondary xylem that were distinctly different from the pattern described for white rot. The first signs of cell wall degradation became evident in the libriform fibres, whose structured walls (middle lamella, primary and secondary cell wall) corresponded to the general pattern of this cell type. Of particular importance for the characterization of the degradation pattern was the thickened secondary cell walls of the libriform fibres, with S<sub>1</sub>, S<sub>2</sub>, and S<sub>3</sub> layers, generally composed of cross-linked cellulose, hemicellulose, lignin, and pectins in varying ratios (Plomion *et al.*, 2001; Schuetz *et al.*, 2013; Rathgeber *et al.*, 2016; Schneider *et al.*, 2017). In the S<sub>2</sub> layers of woody plants, helically arranged cellulose fibrils predominate in most species. The round caverns found here in the S<sub>2</sub> layer of libriform fibres at the periphery of lesions did not correspond either selective delignification or simultaneous degradation of all cell wall components, but were typical of soft rots (Schwarze *et al.*, 1995; Worrall *et al.*, 1997; Schwarze and Fink, 1998; Schwarze, 2007). In the initial stage of lesions, the cavities extended at an acute angle to the long axis, a conclusive indication that initially the helically oriented cellulose fibrils in the S<sub>2</sub> layers were preferentially degraded, as is typical for soft rot (Schwarze, 2007; Schneider *et al.*, 2017). The completely eroded S<sub>2</sub>-layers at the advanced stage also indicated soft rot, as the more lignified components of the cell walls such as the middle lamella, the primary cell walls, the S<sub>1</sub> layer and the inner S<sub>3</sub> layer, remained intact. In the final stage, the more lignified parts of the cell walls, such as the middle lamella, the primary and the S<sub>1</sub> and S<sub>3</sub> lay-

ers of the secondary cell walls, were also affected, while the vessels and tracheids remained intact for longer. Complete disintegration of all xylem elements including VACs and RP in the centres of lesions can be attributed to simultaneous degradation of lignocellulose in the final stage of white rot, as described by Blanchette (1984) and Schwarze (2007).

The existing classification of Esca affected trunks into white rot does not adequately reflect the decomposition pattern observed in the present study, in particular since the binary classification into white rot and brown rot has recently been further developed in favour of a differentiated classification of wood decay mechanisms. It has been proposed that the molecular patterns of enzymes expressed by wood decomposing fungi, such as carbohydrate active enzymes (CAZymes), peroxidases (PODs), and laccases, should be used to characterize decomposition patterns (Riley *et al.*, 2014; Schilling *et al.*, 2015, 2020). These current models show a gradient between phenotypes in which lignin degrading PODs with high selectivity for lignin predominate, and those with high activity of CAZymes, which are highly selective for carbohydrates. Based on the enzyme machinery described in publications on lignocellulose-degrading fungi (Bruno and Sparapano 2006a, Alfaro *et al.* 2014, Ohm *et al.* 2014, Riley *et al.* 2014, Floudas *et al.* 2015, Morales-Cruz *et al.* 2015, Massonette *et al.* 2018a; b; Hage and Rosso 2021), and the microscopic analysis of the degradation pattern described in the present paper, it can be concluded that the lesions caused by Fmed are the result of a transition from soft rot to white rot. The sequence of decomposition steps observed here suggests sequential activity of lignocellulose-degrading enzymes in the course of host tissue colonization by Fmed. Future studies should verify whether Fmed and related Esca pathogens first engage CAZymes to utilize the readily degradable cellulose in the S<sub>2</sub> cell wall layer as resources for subsequent depolymerization of the more persistent lignin by PODs and laccases.

A distinctly different pattern was seen in the lesions with brown spots or streaks, which are clearly attributed to brown wood streaking. Microscopic analysis of the spots showed no evidence of intensive degradation in the cell walls of vessels, tracheids, and libriform fibres, even though lignocellulose-degrading enzymes have been found in pathogens that cause brown wood streaking, such as *D. seriata* and *N. parvum* (Czemmel *et al.*, 2015; Morales-Cruz *et al.*, 2015; Fischer *et al.*, 2016; Stempien *et al.*, 2017; Massonnet *et al.*, 2018 a; b; Garcia *et al.*, 2021). These results indicate that the pathogens use the cell wall lignocellulose as a nutrient substrate to a minor extent. Rather, the presence of hyphae

in the parenchyma of the lesions indicates exploitation of alternative carbon sources in living cells. The clusters of putative amylases and plant invertases found in the *N. parvum* genome (Czemmel *et al.*, 2015) imply that Pch also abundantly degrades starch stored as a reserve in the parenchyma of wood rays. The extent of brown wood streaking from top to bottom, which is limited to small vessel groups or individual vessels, is evidence that the causing agent spread in the vascular system primarily in an axial direction. These observations are in accordance with those of Bruez *et al.* (2020), who suggested top-to-bottom spread of Pch in grapevine trunks. Vessels are grouped into functional vascular bundles forming individual leaf tracks extending through stems and corresponding shoots into the leaves (Pratt 1974; von Arx *et al.*, 2013). Consequently, a vascular bundle with brown wood streaking is in direct contact with a particular shoot and its associated leaves in the host canopy. In this way, toxic or stress-inducing metabolites, and effectors secreted by Esca pathogens in the affected vascular bundles, can be transported *via* the individual leaf track into the corresponding shoots and leaves. This explains the observation, at least in the early stages of GLSD, that symptoms often occur only on single shoots. The scattered single brown stained vessels in secondary xylem can be assigned to brown wood streaking, although they were not visible macroscopically. Lack of visibility also explains the results of Vaz *et al.* (2020), who detected Pch and other agents of brown wood streaking in apparently intact wood, using  $\mu$ -CT analyses.

The obstruction of vessels by tyloses in both white rot and brown wood streaking has also been described by previous authors (Troccoli *et al.*, 2001; Del Rio *et al.*, 2001; Edwards *et al.*, 2007; Mutawila *et al.*, 2011; Fischer and Kassemeyer, 2012; Pouzoulet *et al.*, 2014; Gomez *et al.*, 2016; Pouzoulet *et al.*, 2017; Jacobsen *et al.*, 2018; Bortolami *et al.*, 2019; 2021; Claverie *et al.*, 2020). Tyloses are, among other functions, also respond to abiotic and biotic stress in secondary xylem, and have also been observed in grapevine in response to other vascular colonizing pathogens such as bacteria (Sun *et al.*, 2006; 2008; 2017; Leśniewska *et al.*, 2017; Kashyap, 2021). Massonnet *et al.* (2017) showed that infection of grapevine trunks by *Neofusicoccum parvum* triggered a defense response in the leaves, so this may also occur in the secondary xylem colonized by the pathogens.

The dark discoloration of the demarcations encircling white rot, and the vessels affected by brown wood streaks caused by inclusions of phenolics in the cell lumina, can be considered as defense responses in host tissues. Phenols are generally expressed in host-pathogen interactions by inducing transcriptional and biosynthetic

machinery of the phenylpropanoid pathway, and these compounds serve a number of functions in plant innate immunity (Boller and Felix 2009; Yadav *et al.*, 2021). As a result, numerous hydroxycinnamic acids, stilbenes, and high molecular weight condensation products accumulate in affected xylem (Troccoli *et al.*, 2001, Del Rio *et al.*, 2004; Bruno and Sparapano, 2006b; 2007; Agrelli *et al.*, 2009; Amalfitano *et al.*, 2011; Mutawila *et al.*, 2011; Lambert *et al.*, 2012; 2013; Calzarano *et al.*, 2016; Gómez *et al.*, 2016; Pierron *et al.*, 2016; Rusjan *et al.*, 2017; Spagnolo *et al.*, 2017; Stempien *et al.*, 2017; Khattab *et al.*, 2020; Labois *et al.*, 2020; 2021). Whether the demarcation lines described here in white rot were solely due to a host response to the pathogen, or whether melanized hyphae of the pathogen also accumulate, could not be clarified.

The present anatomical study of Esca-affected trunks has shown that analysis of structural changes using microscopy contributes to a deeper understanding of the molecular and biochemical processes in Esca host-pathogen interactions. Therefore, for complete elucidation of the etiology of Esca, including GLSD, host and pathogen structural interactions must be considered along with the molecular and biochemical aspects of this pathosystem.

## CONCLUSIONS

Comparing the colonization and degradation patterns of the two pathosystems Fmed and Pch in grapevine, fundamental differences between the two emerged. The largely open vascular system in grapevine trunks enables dynamic adaxial pathogen spread direction from top to bottom. In the network of xylem elements, a dense system of pits facilitates lateral spread of Fmed, causing extensive white rot lesions. Cell wall decomposition in the xylem by Fmed indicates an intermediate pattern. Initial soft rot with predominant cellulose decomposition is followed by white rot with simultaneous breakdown of the lignocellulose. Since the final stage of secondary xylem infection by Fmed and related pathogens resembles typical white rot, this term may be further used for this trunk symptom of Esca. In lesions caused by Fmed, there was clear compartmentalization with demarcation zones separating intact secondary xylem from tissues progressively decayed by soft rot first, and then by white rot. This is in accordance with the CODIT model (Compartmentalization of Damage/Dysfunction in Trees), which relates primarily to defense responses against wood-destroying pathogens in the secondary xylem of trees (Shigo 1984, Morris *et al.*, 2016b;

2020). Further studies at structural, biochemical and molecular levels are required to clarify this intermediate status of the degradation pattern of Fmed and how it fits into the CODIT model.

The artificial inoculations of wood cores with Pch are evidence for the causal relationship of this pathogen with brown wood streaking. The present study has shown that brown wood streaking in grapevine plants is not a consequence of significant cell wall decomposition, but rather a reaction of host tissues to infection by this pathogen. In order to clarify the role of Pch in the etiology of Esca, particularly GLSD, further in-depth studies are required on the induction of multiple resistance responses in affected xylem areas, and on biosynthesis and acropetal transport of potential stress factors and toxins.

#### ACKNOWLEDGEMENTS

The authors acknowledge the Michael Fischer Julius-Kühn-Institute for providing the cultures of Fmed and Pch. Sabine Diener of the Albert-Ludwigs-Universität Freiburg, Faculty of Environment and Natural Resources, Forest Botany provided excellent preparation of semithin sections for microscopy. This research was partly funded by a grant of the European Innovation Partnership for Agricultural Productivity and Sustainability (EIP-Agri), and funding from the Baden-Württemberg State Ministry for Rural Areas, Nutrition and Consumer Protection.

#### LITERATURE CITED

- Agrelli D., Amalfitano C., Conte P., Mugnai L., 2009. Chemical and spectroscopic characteristics of the wood of *Vitis vinifera* "Sangiovese" affected by esca disease. *Journal of Agricultural and Food Chemistry* 57 (24): 11469–11475. DOI: 10.1021/jf903561x
- Alfaro M., Oguiza J.A., Ramírez L., Pisabarro A.G., 2014. Comparative analysis of secretomes in basidiomycete fungi. *Journal of Proteomics* 102: 28–42. DOI: 10.1016/j.prot.2014.03.001
- Amalfitano C., Agrelli D., Arrigo A., Mugnai L., Surico G., Evidente A., 2011. Stilbene polyphenols in the brown red wood of *Vitis vinifera* "Sangiovese" affected by "esca proper" *Phytopathologia Mediterranea* 50: S224–S235. DOI: 10.14601/Phytopathol\_Mediterr-9720
- Angyalossy V., Angele G., Pace M.R., Lima A.C., Dias-Leme C.L., ... Madero-Vega C., 2012. An overview of the anatomy, development and evolution of the vascular system of lianas. *Plant Ecology & Diversity* 5(2): 167–182. DOI: 10.1080/17550874.2011.615574.
- Baránek M., Armengol J., Holleínová V., Pečenka J., Calzarano F., ... Eichmeier A., 2018. Incidence of symptoms and fungal pathogens associated with grapevine trunk diseases in Czech vineyards: First example from a north-eastern European grape-growing region. *Phytopathologia Mediterranea* 57(3): 449–458. DOI: 10.14601/Phytopathol\_Mediterr-22460.
- Bertsch C., Ramírez-Suero M., Maginin-Robert M., Larignon P., Chong J., ... Fontaine F., 2013. Grapevine trunk diseases: Complex and still poorly understood. *Plant Pathology* 62(2): 243–265. DOI: 10.1111/j.1365-3059.2012.02674.x.
- Blanchette R.A., 1984. Screening wood decay by white rot fungi for preferential lignin degradation. *Applied and Environmental Microbiology* 48(3): 646–653. DOI: 10.1128/aem.48.3.647-653.1984
- Boller T., Felix G., 2009. A renaissance of elicitors: Perception of microbe associated molecular patterns and danger signals by pattern-recognition receptors. *Annual Review of Plant Biology* 60: 379–406. DOI: 10.1146/annurev.arplant.57.032905.105346
- Bortolami G., Gambetta G.A., Delzon S., Lamarque L.J., Pouzoulet J., ... Delmas C.E.L., 2019. Exploring the hydraulic failure hypothesis of esca leaf symptom formation. *Plant Physiology* 181: 1163–1174. DOI: 10.1104/pp.19.00591
- Bortolami G., Farolfi E., Badel E., Burlett R., Cochard H., ... Delmas C.E.L., 2021. Seasonal and long-term consequences of esca grapevine disease on stem xylem integrity. *Journal of Experimental Botany* 72(10): 3914–3928. DOI: 10.1093/jxb/erab117.
- Brown A.A., Lawrence D.P., Baumgartner K., 2020. Role of basidiomycete fungi in the grapevine trunk disease esca. *Plant Pathology* 69(2): 205–220. DOI: 10.1111/ppa.13116.
- Bruez E., Vallance J., Gerbore J., Lecomte P., Da Costa J.P., ... L., Rey P., 2014. Analyses of the temporal dynamics of fungal communities colonizing the healthy wood tissue of esca leaf-symptomatic and asymptomatic vines. *PLoS ONE* 9(5): e5928. DOI: 10.1371/journal.pone.0095928.
- Bruez E., Baumgartner K., Bastien S., Travadon R., Guérin-Dubravna L., Rey P., 2016. Various fungal communities colonise the functional wood. *Australian Journal of Grape and Wine Research* 22: 288–295. DOI: 10.1111/ajgw.12209
- Bruez E., Vallance J., Gautier A., Laval V., Compant S., ... Rey P., 2020. Major changes in grapevine wood microbiota are associated with the onset of esca, a devastating trunk disease. *Environmental Micro-*

- biology* 22(12): 5189–5206. DOI: 10.1111/1462-2920.15180.
- Bruno G., Sparapano L., 2006a. Effects of three esca-associated fungi on *Vitis vinifera* L.: III Enzymes produced by the pathogens and their role in fungus-to-plant or in fungus-to-fungus interactions. *Physiological and Molecular Plant Pathology* 69: 182–194. DOI:10.1016/j.pmp.2007.04.006
- Bruno G., Sparapano L., 2006b. Effects if three esca-associated fungi on *Vitis vinifera* L.: II. Characterization of biomolecules in xylem sap and leaves of healthy and diseased vines. *Physiological and Molecular Plant Pathology* 69: 195–208. DOI: 10.1016/j.pmp.2007.04.007.
- Bruno G., Sparapano L., 2007. Effects if three esca-associated fungi on *Vitis vinifera* L.: V. Changes in the chemical and biological profile of xylem sap from diseased “Sangiovese”. *Physiological and Molecular Plant Pathology* 71: 210–229. DOI: 10.1016/j.pmp.2008.02.005.
- Calzarano F., D’Agostino V., Pepe A., Osti F., Della Pelle F., ... Di Marco S., 2016. Patterns of phytoalexins in the grapevine leaf stripe (esca complex) / grapevine pathosystem. *Phytopathologia Mediterranea* 55: 410–426. DOI: 10 (3):14601/Phytopathol\_Mediterr-18681.
- Carlquist S., 1985. Observations on functional wood histology of vine and lianas: Vessel dimorphism, tracheids, narrow vessels and parenchyma. *Aliso* 11(2): 139–157. <https://scholarship.claremont.edu/aliso/vol11/iss2/3>
- Carlquist S., 2010 Comparative wood anatomy. *Systematic, Ecological and Evolutionary Aspects of Dicotyledone Wood*. 2<sup>nd</sup> ed. Springer series in wood science Springer-Verlag Heidelberg. Germany SSN 1431-8563-0.
- Carlquist S., 2012. How wood evolves: a new synthesis. *Botany* 90: 901–940. DOI:10.1139/B2012-048
- Claverie M., Notaro M., Fontaine F., Wery J., 2020. Current knowledge on grapevine trunk diseases with complex etiology: A systemic approach. *Phytopathologia Mediterranea* 59(1): 29–53. DOI: 10.14601/Phyto-11150
- Chiarappa L., 2000. Esca (black measles) of grapevine. An overview. *Phytopathologia Mediterranea* 39(1): 11–15. DOI: 10.14601/Phytopathol\_Mediterr-1537
- Cloete M., Mostert L., Fischer M., Halleen F., 2015. Pathogenicity of South African *Hymenochaetales* taxa isolated from esca-infected grapevines. *Phytopathologia Mediterranea* 54(2): 368–379. DOI: 10.14601/Phytopathol\_Mediterr-16237
- Cortesi P., Fischer M., Milgroom M.G., 2000. Identification and spread of *Fomitiporia punctata* associated with wood decay of grapevine showing symptoms of esca. *Phytopathology* 90(9): 967–972. DOI: 10.1094/PHYTO.2000.90.9.967
- Crous P.W., Gams W., 2000. *Phaeomoniella chlamydospora* gen. et comb. nov., a causal organism of Petri grapevine decline and esca. *Phytopathologia Mediterranea* 39(1): 112–118. DOI:10.14601/Phytopathol\_Mediterr-1530
- Crous P.W., Slippers B., Wingfield M.J., Rheeder J., Marasas W.F.O., ... Groenewald J.Z., 2006. Phylogenetic lineages in the *Botryosphaeriaceae*. *Studies in Mycology* 55: 235–253.
- Czemmel S., Gaarneau E.R., Travadon R., McElrone A.J., Cramer G.R., Baumgartner K., 2015. Genes expressed on grapevine leaves reveal latent wood infection by the fungal pathogen *Neofusicoccum parvum*. *PLoS ONE* 10: e0121828. DOI: 10.1371/journal.pone.0121828.
- Daniel G., Volc J., Niku-Paavola M.L., 2004. Cryo-FE-SEM and TEM immuno-techniques reveal new details for understanding white-rot decay of lignocellulose. *Comptes Rendus Biologies* 327: 861–871. DOI: 10.1016/j.crv.2004.08.003
- Daniel G., 2014. Fungal and bacterial biodegradation: White rots, brown rots, soft rots and bacteria. In: *Deterioration and Protection of Sustainable Biomaterial ACS Symposium Series* (Schultz T.P., Godell B., Nocholas D.D., ed.). pp. 24–58. American Chemical Society, Washington DC, 23–58.
- Del Frari G., Gobbi A., Aggerbeck M.R., Oliveira H., Hansen L.H., Ferreira R.B., 2019. Characterization of the wood microbiome of *Vitis vinifera* in a vineyard affected by esca. Spatial distribution of fungal communities and their putative relation with leaf symptoms. *Frontier in Plant Science* 10: 910. DOI: 10.3389/fpls.2019.00910.
- Del Frari, G., Oliveira, H., Boavida Ferreira, R., 2021. White Rot Fungi (*Hymenochaetales*) and esca of grapevine: Insights from recent microbiome Studies. *Journal of Fungi* 7: 770. DOI: 10.3390/jof7090770
- Del Rio J.A., Gómez P., Baidez A., Fuster M.D., Ortuño A., 2001. Tylose formation and changes in phenolic compounds of grape roots infected with *Phaeomoniella chlamydospora* and *Phaeoacremonium* species. *Phytopathologia Mediterranea*. 40(1): S394–S399. DOI: 10.14601/Phytopathol\_Mediterr-1644
- Del Rio J.A., Gómez P., Báidez A., Fuster D.M., Ortuño, Frias V., 2004. Phenolic compounds have a role in the defence mechanism protecting grapevine against the fungi involved in Petri disease. *Phytopathologia Mediterranea* 43(1): 87–94. DOI: 10.14601/Phytopathol\_Mediterr-1736

- Donaldson L.A., Cairns M., Hilla S.J., 2018. Comparison of micropore distribution in cell walls of softwood and hardwood xylem. *Plant Physiology* 178: 1142–1153. DOI:10.1104/pp.18.00883
- Edwards J., Pascoe. I.G., Salib S., 2007. Impairment of grapevine xylem function by *Phaeoconiella chlamydospora* infection is due to more than physical blockage of vessels with 'goo'. *Phytopathologia Mediterranea* 46(1): 87–90. DOI: 10.14601/Phytopathol\_Mediterr-1858
- Elena G., Bruez E., Rey P., Luque J., 2018. Microbiota of grapevine woody tissues with or without esca-foliar symptoms in northeast Spain. *Phytopathologia Mediterranea* 57(3): 425–438. DOI: 10.14601/Phytopathol\_Mediterr-23337
- Fischer J., Compant S., Pierron R.J.G., Gorfer M., Jacques A., ... Berger H., 2016. Differing alterations of two esca associated fungi, *Phaeoacremonium aleophilum* and *Phaeoconiella chlamydospora* on transcriptomic level, to co-cultured *Vitis vinifera* L. calli. PLoS ONE 11(9): e0163344. DOI:10.1371/journal.pone.0163344
- Fischer M., 2001. A new wood-decaying basidiomycete species associated with esca of grapevine: *Fomitiporia mediterranea* (Hymenochaetales). *Mycological Progress* 13(3): 315–324. DOI: 10.1007/s11557-006-0029-4
- Fischer M., and Kassemeyer H.H., 2003. Fungi associated with esca disease of grapevine in Germany. *Vitis* 42(3): 109–116. DOI: 10.5073/vitis.2003.42.109-116
- Fischer M., and Kassemeyer H.H., 2012. Water regime and its possible impact on expression of esca symptoms in *Vitis vinifera*: Growth characters and symptoms in the greenhouse after artificial infection with *Phaeoconiella chlamydospora*. *Vitis* 51(3): 129–135. DOI 10.5073/vitis.2012.51.129-135
- Fischer M., and Peighami Ashnaei S. 2019. Grapevine, esca complex, and environment: The disease triangle *Phytopathologia Mediterranea* 58(1): 17–37. DOI: 10.14601/Phytopathol\_Mediterr-25086
- Floudas D., Benjamin W., Held B.W., Riley R., Nagy L.G., ... Hibbett D.S., 2015. Evolution of novel wood decay mechanisms in *Agaricales* revealed by the genome sequences of *Fistulina hepatica* and *Cylindrobasidium torrendii*. *Fungal Genetics and Biology* 76: 78–92. DOI: 10.1016/j.fgb.2015.02.002
- Gallenmüller F. Müller U., Rowe N., Speck T., 2001. The Growth Form of *Croton pullei* (Euphorbiaceae) - Functional Morphology and Biomechanics of a Neotropical Liana. *Plant Biology* 3: 50–61. DOI: 10.1055/s-2001-11750
- Gao Y., Yang Z., Wang G., Sun J., Zhang X., 2020. Discerning the difference between lumens and scalariform perforation plates in impeding water flow in single xylem vessels and vessel networks in cotton. *Frontiers in Plant Science* 11: 246. DOI: 10.3389/fpls.2020.00246
- Garcia J.F., Lawrence D.P., Morales-Cruz A., Travadon R., Minio A., ... Cantu D., 2021. Phylogenomics of plant-associated *Botryosphaeriaceae* species. *Frontiers in Microbiology* 12: 652802. DOI: 10.3389/fmicb.2021.652802
- Gómez P., Báidez A.G., Ortuño A., Del Río J.A., 2016. Grapevine xylem response to fungi involved in trunk diseases. *European Journal of Plant Pathology* 169: 116–124. DOI: 10.1111/aab12285
- Goodell B., Quian Y., Jellison J., 2008. Fungal decay of wood: Soft rot-brown rot – white rot. *ACS Symposium Series* 82: 9–31. DOI: 10.1021/bk-2008-0982.ch002
- Gramaje D., Úrbez-Torres J.R., Sosnowski M.R., 2018. Managing grapevine trunk diseases with respect to etiology and epidemiology: Current strategies and future prospects. *Plant Disease* 102(1): 12–39. DOI: 10.1094/pdis-04-17-0512-fe
- Guerin-Dubrana L., Fontaine F, Mugnai L., 2019. Grapevine trunk disease in European and Mediterranean vineyards: Occurrence, distribution and associated disease-affecting cultural factors. *Phytopathologia Mediterranea* 58(1): 49–71. DOI: 10.14601/Phytopathol\_Mediterr-25153
- Hacke U.G., Sperry J.S., 2001. Functional and ecological xylem anatomy. *Perspectives in Plant Ecology, Evolution and Systematics* 4(2): 97–115. DOI: 10.1078/1433-8319-00017
- Hage H., Rosso M.N., 2021. Evolution of Fungal Carbohydrate-Active Enzyme Portfolios and Adaptation to Plant Cell-Wall Polymers. *Journal of Fungi* 7: 185. DOI: 10.3390/jof7030185
- Haidar R., Yacoub A., Vallance J., Compant S., Antonielli L., ... Rey P., 2021. Bacteria associated with wood tissues of esca-diseased grapevines: functional diversity and synergy with *Fomitiporia mediterranea* to degrade wood components. *Environmental Microbiology* 23(10): 6104–6121. DOI:10.1111/1462-2920.15676
- Hastrup A.C.S., Howell C., Larsen F.H., Sathitsuksanoh N., 2012. Differences in crystalline cellulose modification due to degradation by brown and white rot fungi. *Fungal Biology* 116: 1052–1063. DOI: 10.1016/j.funbio.2012.07.009.
- Hess J., Balasundaram S.V., Bakkemo R.I., Drula E., Henrissat B., ... Skrede I., 2020. Niche differentiation and evolution of the wood decay machinery in the invasive fungus *Serpula lacrymans*. *The ISEM Journal* 15: 592–604. DOI: 10.1038/s41396-020-00799-5

- Hofstetter V., Buyck B., Croll D., Viret O., Couloux A., Gindro K., 2012. What if esca disease of grapevine were not a fungal disease? *Fungal Diversity* 54: 51–67. DOI 10.1007/s13225-012-0171-z
- Holbroock N.M., Zwieniecki M.A., 1999. Embolism repair and xylem tension: Do we need a miracle. *Plant Physiology* 120: 7–10. DOI: 10.1104/pp.120.1.7
- Hrycan J., Hart M., Bowen P., Forge T., Úrbez-Torres J.R., 2020. Grapevine trunk disease fungi: Their roles as latent pathogens and stress factors that favour disease development and symptom expression. *Phytopathologia Mediterranea* 59(3): 395–424. DOI: 10.14601/Phyto-11275
- Jacobsen A. L., Valdovinos-Ayala J., Pratt R.B., 2018. Functional lifespans of xylem vessels: Development, hydraulic function, and post-function of vessels in several species of woody plants. *American Journal of Botany* 105(2): 142–150. DOI:10.1002/ajb2.1029
- Kaack L., Weber M., Isasa E., Karimi Z., Li S., ... Jansen S., 2021. Pore constrictions in intervessel pit membranes provide a mechanistic explanation for xylem embolism resistance in angiosperms. *New Phytologist* 230: 1829–1843. DOI: 10.1111/nph.17282
- Kashyap A., Planas-Marques M., Capellades M., Valls M., Coll N.S., 2021. Blocking intruders: inducible physico-chemical barriers against plant vascular wilt pathogens. *Journal of Experimental Botany* 72(2): 184–198. DOI:10.1093/jxb/eraa444
- Khattab I.M., Sahi V.P., Baltenweck R., Maia-Grondard A., Huguency P., ... Nick P., 2020. Ancestral chemotypes of cultivated grapevine with resistance to *Botryosphaeriaceae*-related dieback allocate metabolism towards bioactive stilbenes. *New Phytologist* 229: 1133–1146. DOI: 10.1111/nph.16919
- Kedrov G.B., 2013. Scalariform tracheids in secondary xylem of woody dicotyledons: Distribution, function and evolutionary significance. *Wulfenia* 20: 43–54
- Koddenberg T., Greving I., Hagemann J., Flenner S., Krause A., ... Nopens M., 2021. Threedimensional imaging of xylem at cell wall level through near field nano holotomography. *Nature Scientific Reports* 11: 4574. DOI: 10.1038/s41598-021-83885-8
- Koyani R.D., Sanghvi G.V., Bhatt I.M., Rajput K.S., 2010. Pattern of delignification in *Ailanthus excelsa* Roxb. Wood by *Inonotus hispidus* (Bull.: Fr.) Karst. *Mycology* 1(3): 204–211. DOI 10.1080/21501203.2010.5.516409
- Labois C., Wilhelm K., Laloue H., Tarnus C., Bertsch C., Goddard M.L., Chong J., 2020. Wood metabolomics response of wild and cultivated grapevine to infection with *Neofusicoccum parvum*, a trunk disease pathogen. *Metabolites* 10: 232. DOI: 10.3390/metabo10060232
- Labois C., Stempien E., Schneider J., Schaeffer-Reiss C., Bertsch C., Goddard M.-L., Chong J., 2021. Comparative study of secreted proteins, enzymatic activities of wood degradation and stilbene metabolism in grapevine *Botryosphaeria* dieback fungi. *Journal of Fungi* 7: 568. DOI:10.3390/jof7070568
- Lambert C., Bisson J., Waffo-Téguo P., Papastamoulis Y., Richard T., ... Cluzet S., 2012. Phenolics and their antifungal role in grapevine wood decay: Focus on the *Botryosphaeriaceae* family. *Journal of Agricultural and Food Chemistry* 60: 11859–11868dx. DOI: 10.1021/jf303290g
- Lambert, C., Khiook, I. L. K., Lucas, S., Téléf-Micouleau, N., Mérillon, J.-M., Cluzet, S., 2013. A faster and a stronger defense response: One of the key elements in grapevine explaining its lower level of susceptibility to esca? *Phytopathology* 103: 1028–1034. DOI: 10.1094/PHYTO-11-12-0305-R
- Larignon P., Dubos B., 1997. Fungi associated with esca disease in grapevine. *European Journal of Plant Pathology* 103: 147–157. DOI: 10.1023/A:1008638409410
- Larsson K.H., Parmasto E., Fischer M., Langer E., Nakasone K.K., Redhead S.A., 2006. *Hymenochaetales*: a molecular phylogeny for the hymenochaetoid clade. *Mycologia* 98(6): 926–936. DOI: 10.3852/mycologia.98.6.926
- Lecomte P., Darrietort G., Liminana J.-M., Comont G., Muruamendiaraz A., ... Fermaud, M., 2012. New insights into esca of grapevine: The development of foliar symptoms and their association with xylem discoloration. *Plant Diseases* 96: 924–934. DOI: 10.1094/PDIS-09-11-0776-RE
- Leśniewska J., Öhmann D., Krzesłowska M., Kushwa S., Barciszewska-Pacak M., ... Mellerowicz E.J., 2017. Defense response in aspen with altered pectin methylesterase activity reveal the hormonal inducers of tylosis. *Plant Physiology* 173: 1409–1419. DOI: 10.1104/pp.16.01443
- Li S., Bonneau F., Chadoeuf J., Picart D., Gégout-Petit A., Guérin-Dubrana L., 2017. Spatial and temporal pattern analyses of esca grapevine disease in vineyards in France. *Phytopathology* 107: 59–69. DOI: 10.1094/PHYTO-07-15-0154-R
- Liers C., Arnstadt T., Ullrich R., Hofrichter M., 2011. Patterns of lignin degradation and oxidative enzyme secretion by different wood- and litter-colonizing *Basidiomycetes* and *Ascomycetes* grown on beechwood. *FEMS Microbiology Ecology* 78: 91–102. DOI:10.1111/j.1574-6941.2011.01144.x
- Lima M.R.M., Machado A.F., Gubler W.D., 2017. Metabolomic studies of “Chardonnay” grapevine double

- stressed with esca-associated fungi and drought. *Phytopathology* 107: 669–680. DOI: 10.1094/PHYTO-11-26-0410-R
- Trocchi T., Calamassi R., Mori B., Mugnai L., Surico G., 2001. *Phaeoconiella chlamydospora*-grapevine interaction: Histochemical reactions to fungal infection. *Phytopathologia Mediterranea* 40: S400–S406. DOI: 10.14601/Phytopathol\_Mediterr-1610
- Maher N., Piot J., Bastien S., Vallance J., Rey P., Guérin-Dubrana J., 2011. Wood necrosis in esca-affected vines. Types, relationship and possible links with foliar symptom expression. *Journal International des Sciences de la Vigne et du Vin* 46(1):15–27. DOI:10.20870/oeno-one.2012.46.1.1507
- Martinez-Diz M.P., Eichmeier A., Spetik M., Bujanda R., Díaz-Fernández A., ... Gramaje D., 2020. Grapevine pruning time affects natural wound colonization by wood invading fungi. *Fungal Ecology* 48: 1–13. DOI: 10.1016/j.funeco.2020.100994
- Masi M., Cimmino A., Reveglia P., Mugnai L., Surico G., Evidente A., 2018. Advances on fungal phytotoxins and their role in grapevine trunk diseases. *Journal of Agricultural and Food Chemistry* 66(5): 948–958. DOI: 10.1021/acs.jafc.8b00773.
- Masselter T., Speck T., 2008. Quantitative and qualitative changes in primary and secondary stem organization of *Aristolochia macrophylla* during ontogeny: Functional growth analysis and experiments. *Journal of Experimental Botany* 59(11): 2955–2967. DOI:10.1093/jxb/ern151
- Massonnet M., Figueroa-Balderas R., Galarneau E.R.A., Miki S., Lawrence D.P., ... Cantu D., 2017. *Neofusicoccum parvum* colonization of the grapevine woody stem triggers asynchronous host responses at the site of infection and in the leaves. *Frontier in Plant Science* 8: 1117. DOI: 10.3389/fpls.2017.01117
- Massonnet M., Morales-Cruz A., Figueroa-Balderas R., Lawrence D.P., Baumgartner K., Cantu D., 2018a. Condition-dependent co-regulation of genomic clusters of virulence factors in the grapevine trunk pathogen *Neofusicoccum parvum*. *Molecular Plant Pathology* 19: 21–34 DOI: 10.1111/mpp.12491
- Massonnet M., Morales-Cruz A., Minio A., Figueroa-Balderas R., Lawrence D.P., ... Cantu D., 2018b. Whole-genome resequencing and pan-transcriptome reconstruction highlight the impact of genomic structural variation on secondary metabolite gene clusters in the grapevine esca pathogen *Phaeoacremonium minimum*. *Frontiers in Microbiology* 9: 1784. DOI: 10.3389/fmicb.2018.01784
- Miedes E., Vanholme R., Boerjan W., Molina A., 2014. The role of the secondary cell wall in plant resistance to pathogens. *Frontiers in Plant Science* 5: 358. DOI: 10.3389/fpls.2014.00358
- Mondello V., Songy A., Battiston E., Pinto C., Coppin C., ... Fontaine F., 2018. Grapevine trunk diseases: A review of fifteen years of trials for their control with chemicals and biocontrol agents. *Plant Disease* 10: 1189–1217. DOI: 10.1094/PDSI-08-17-1181-FE
- Morales-Cruz A., Amrine K.C.H., Blanco-Ulate B., Lawrence D.P., Travadon R., ... Cantu D., 2015. Distinctive expansion of gene families associated with plant cell wall degradation, secondary metabolism, and nutrient uptake in the genomes of grapevine trunk pathogens. *BMC Genomics* 16: 469. DOI 10.1186/s12864-015-1624-z
- Moretti S., Pacetti A., Pierron R., Kassemeyer H.H., Fischer M., ... Farine S., 2021. *Fomitiporia mediterranea* M. Fisch., the historical esca agent: A comprehensive review on the main grapevine wood rot agent in Europe. *Phytopathologia Mediterranea* 60 (2): 357–385. DOI: 10.14601/Phyto-13021
- Morgenstern I., Robertson D.L., Hibbett D.S., 2010. Characterization of three *mnp* genes of *Fomitiporia mediterranea* and report of additional class II peroxidases in the order *Hymenochaetales*. *Applied and Environmental Microbiology* 76(19): 6431–6440. DOI:10.1128/AEM.00547-10
- Morris H., Jansen S., 2016. Secondary xylem parenchyma – From classical terminology to functional traits. *IAW Journal* 37(1): 1–13. DOI: 10.1163/22941932-201160117
- Morris H., Plavcová L., Cvecko P., Fichtler E., Gillingham M.A.F., ... Jansen S., 2016 a. A global analysis of parenchyma tissue fractions in secondary xylem of seed plants. *New Phytologist* 209: 1553–1565. DOI: 10.1111/nph.13737
- Morris H., Brodersen C., Schwarze F.W.M.R., Jansen S., 2016b. The parenchyma of secondary xylem and its critical role in tree defense against fungal decay in relation to the CODIT model. *Frontiers in Plant Science* 7: 1665. DOI: 10.3389/fpls.2016.01665
- Morris H., Plavcova L., MGorai M., Klepsch M., Kotowska M., ... Jansen S., 2018. Vessel-associated cells in angiosperm xylem: Highly specialized living cells at the symplast–apoplast boundary. *American Journal of Botany* 105(2): 151–160. DOI:10.1002/ajb2.1030
- Morris H., Hietala A.M., Jansen S., Ribera J., Rosner S., ... Schwarze F.W.M.R., 2020. Using the CODIT model to explain secondary metabolites of xylem in defence systems of temperate trees against decay fungi. *Annals of Botany* 125(5): 701–720. DOI: 10.1093/aob/mcz138
- Mugnai L., Graniti A., Surico G., 1999. Esca (Black measles) and brown wood-streaking: Two old and elusive

- diseases of grapevine. *Plant Disease* 83(5): 404–418. DOI: 10.1094/PDIS.1999.83.5.404
- Mutawila C., Fourie P., Halleen F., Mostert L., 2011. Histo-pathology study of the growth of *Trichoderma harzianum*, *Phaeoconiella chlamydospora* and *Eutypa lata* on grapevine pruning wounds. *Phytopathologia Mediterranea* 50: S46–S60.
- Ohm R.A., Riley R., Salamov A., Min B., Choi I.G., Grigoriev I.V., 2014. Genomics of wood-degrading fungi. *Fungal Genetics and Biology* 72: 82–90. DOI: 10.1016/j.fgb.2014.05.001
- Pacetti A., Moretti S., Pinto C., Compant S., Farine S., ... Mugnai L., 2021. Trunk surgery as a tool to reduce foliar symptoms in diseases of the esca complex and its influence on vine wood microbiota. *Journal of Fungi*: 7(7), 521. DOI: 0.3390/jof7070521
- Pacetti A., Moretti S., Perrin C., Gelhaye E., Bieler E., ... Bertsch C., 2022. Grapevine wood-wegrading activity of *Fomitiporia mediterranea* M. Fisch.: A focus on the enzymatic pathway regulation. *Frontiers in Microbiology* 13: 844264. DOI: 10.3389/fmicb.2022.844264. PMID: 35369524; PMCID: PMC8971955.
- Pacifico D., Squartini A., Crucitti D., Barizza E., Lo Schiavo F., ... Zottini M., 2019. The role of the endophytic microbiome in the grapevine response to environmental triggers. *Frontiers in Plant Science* 10: 1256. DOI: 10.3389/fpls.2019.01256
- Pfautsch S., Hölttä T., Mencuccini M., 2015 a. Hydraulic functioning of tree stems - fusing ray anatomy, radial transfer and capacitance. *Tree Physiology* 35: 706–722. DOI:10.1093/treephys/tpv058
- Pfautsch S., Renard J., Tjoelker M.G., Salih A., 2015 b. Phloem as capacitor: Radial transfer of water into xylem of tree stems occurs via symplastic transport in ray parenchyma. *Plant Physiology* 167: 963–971. DOI: 10.1104/pp.114.254581
- Pierron R.J.G., Pouzoulet J., Couderc C., Judic E., Compant S., Jacques A., 2016. Variations in early response of grapevine wood depending on wound and inoculation combinations with *Phaeoacremonium aleophilum* and *Phaeoconiella chlamydospora*. *Frontiers- in. Plant Science* 7: 268. DOI: 10.3389/fpls.2016.00268
- Plomion C., Leprovost G., Stokes A., 2001. Wood formation in trees. *Plant Physiology* 127: 1513–1523. DOI: 10.1104/pp.010816
- Pouzoulet J., Pivovarov A.L., Santiago L.S., Rolshausen P.E. 2014. Can vessel dimension explain tolerance toward fungal vascular wilt diseases in woody plants? Lessons from Dutch elm disease and esca disease in grapevine. *Frontiers in Plant Science* 5: 253. DOI: 10.3389/fpls.2014.00253
- Pouzoulet J., Scudiero E., Schiavon M., Rolshausen P.E. 2017. Xylem vessel diameter affects the compartmentalization of the vascular pathogen *Phaeoconiella chlamydospora* in grapevine. *Front. Plant Sci.* 8: 1442. DOI: 10.3389/fpls.2017.01442
- Pouzoulet J., Rolshausen P.E., Charbois R., Chen J., Guillaumie S., ... Delmas C.E.L., 2020. Behind the curtain of the compartmentalization process: Exploring how xylem vessel diameter impacts vascular pathogen resistance. *Plant Cell & Environmen* 43: 2782–2796. DOI: 10.1111/pce.13848
- Pratt C. 1974. Vegetative anatomy of cultivated grapes – A review. *American Journal of. Enology and Viticulture* 25(3): 131–149.
- Rathgeber C.B.K., Cuny H.E., Fonti P., 2016. Biological basis of tree-ring formation: A crash course. *Frontiers in Plant Science* 7: 734. DOI: 10.3389/fpls.2016.00734
- Reis P., Pierron R., Larignon P., Lecomte P., Abou-Mansour E., ... Fontaine F., 2019. *Vitis* methods to understand and develop strategies for diagnosis and sustainable control of grapevine trunk diseases. *Phytopathology* 109: 916–931. DOI: 10.1094/PHYTO-09-18-0349-RVW
- Riley R., Salamov A.A., Brown D.W., Nagy L.G., Floudas D., ... Grigoriev I.V., 2014. Extensive sampling of basidiomycete genomes demonstrates inadequacy of the white-rot/brown-rot paradigm for wood decay fungi. *Proceedings of the National Academy of Sciences (PNAS)* 111(27): 9923–9928. DOI: 10.1073/pnas.1400592111
- Rolshausen P., Úrbez-Torres J.R., Rooney-Latham S., Eskalen A., Smith R.J., Gubler W.G., 2010. Evaluation of pruning wound susceptibility and protection against fungi associated with grapevine trunk diseases. *American Journal o. Enology and Viticulture* 61: 113–119.
- Rowe N., Speck T., 2004. Plant growth forms: An ecological and evolutionary perspective. *New Phytologist* 166: 61–72. Doi: 10.1111/j.1469-8137.2004.01309.x
- Rusjan D., Persic M., Likar M., Biniari K., Mikulic-Petkovsek M., 2017. Phenolic responses to esca-associated fungi in differently decayed grapevine woods from different trunk parts of ‘Cabernet Sauvignon’. *Journal of Agricultural and Food Chemistry* 65: 6615–6624 DOI: 10.1021/acs.jafc.7b02188
- Sano Y., Utsumi Y., Nakada R., 2013. Homoplastic occurrence of perforated pit membranes and torus-bearing pit membranes in ancestral angiosperms as observed by field-emission scanning electron microscopy. *Journal of Wood Science* 59: 95–103. DOI: 10.1007/s10086-012-1304-4
- Schilling J.S., Kaffenberger J.T., Liew F.J., Song Z., 2015. Signature wood modifications reveal decomposer

- community history. *PLoS ONE* 10: e0120679. DOI: 10.1371/journal.pone.0120679
- Schilling J.S., Kaffenberger J.T., Held B.W., Ortiz R., Blanchette R.A., 2020. Using wood rot phenotypes to illuminate the “Gray” among decomposer fungi. *Frontiers in Microbiology* 11: 1288. DOI: 10.3389/fmicb.2020.01288
- Schneider R., Tang L., Lampugnani E.R., Barkwill S., Lathe R., ... Persson A., 2017. Two complementary mechanisms underpin cell wall patterning during xylem vessel development. *The Plant Cell* 29: 2433–2449. DOI: 10.1105/tpc.17.00309
- Schuetz M., Smith R., Ellis B., 2013. Xylem tissue specification, patterning, and differentiation mechanisms. *Journal of Experimental Botany* 64(1): 11–31. DOI: 10.1093/jxb/ers287
- Schwarze F.W.M.R., 2007. Wood decay under the microscope. *Fungal Biology Reviews* 21(4): 133–170. DOI: 10.1016/j.fbr.2007.09.001
- Schwarze F. W. M. R., Fink S. 1998. Host and cell type affect the mode of degradation by *Meripilus giganteus*. *New Phytologist* 139: 721–731. DOI: 10.1046/j.1469-8137.1998.00238.x
- Schwarze F. W. M. R., Lonsdale D., Fink S., 1995. Soft rot and multiple T-branching by the basidiomycete *Inonotus hispidus* in ash and London plane. *Mycological Research*. 99: 813–820. DOI: 10.1016/S0953-7562(09)80732-6
- Secchi F., Pagliarani C., Zwieniecki M.A., 2017. The functional role of xylem parenchyma cells and aquaporins during recovery from severe water stress. *Plant, Cell and Environment* 40: 858–871. DOI: 10.1111/pce.12831
- Shigo A.L., 1984. Compartmentalization: A conceptual framework for understanding how trees grow and defend themselves. *Annual Review of Phytopathology* 22: 189–214.
- Spagnolo A., Mondello V., Larignon P., Villaume S., Rabenoelina F., ... Fontaine F., 2017. Defense responses in grapevine (“Mourvèdre”) after inoculation with the *Botryosphaeria* dieback pathogens *Neofusicoccum parvum* and *Diplodia seriata* and their relationship with flowering. *International Journal of Molecular Science* 18: 393. DOI: 10.3390/ijms18020393
- Stempien E., Goddard M.L., Wilhelm K., Tarnus C., Bertsch C., Chong J., 2017. Grapevine *Botryosphaeria* dieback fungi have specific aggressiveness factor repertory involved in wood decay and stilbene metabolism. *PLoS ONE* 12. DOI: 10.1371/journal.pone.0188766
- Sun Q., Rost T.L., Matthews M.A., 2006. Pruning-induced tylose development in stems of current-year shoots of *Vitis vinifera* (Vitaceae). *American Journal of Botany* 93(11): 1567–1576. DOI: 10.3732/ajb.93.11.1567
- Sun Q., Rost T.L., Matthews M.A., 2008. Wound-induced vascular occlusions in *Vitis vinifera* (Vitaceae). *American Journal of Botany* 95(12): 1498–1505. DOI: 10.3732/ajb.0800061
- Sun Q., Sun Y., Juzenas K., 2017. Immunogold scanning electron microscopy can reveal the polysaccharide architecture of xylem cell walls. *Journal of Experimental Botany*, 68(9): 2231–2244. DOI: 10.1093/jxb/erx103
- Surico G., Marchi G., Braccini P., Mugnai L., 2000. Epidemiology of esca in some vineyards in Tuscany (Italy). *Phytopathologia Mediterranea* 39(1): 190–205. DOI: 10.14601/Phytopathol\_Mediterr-1536
- Surico G., 2009. Towards a redefinition of the diseases within the esca complex of grapevine. *Phytopathologia Mediterranea*. 48(1): 5–10. DOI:10.14601/Phytopathol\_Mediterr-2870
- Travadon, R., Rolshausen, P. E., Gubler, W. D., Cadle-Davidson, L., Baumgartner, K., 2013. Susceptibility of cultivated and wild *Vitis* spp. to wood infection by fungal trunk pathogens. *Plant Disease*. 97: 1529–1536. DOI: 10.1094/PDIS-05-13-0525-RE
- Travadon R., Lecomte P., Diarra B., Lawrence D.P., Renault D., ... Baumgartner K., 2016. Grapevine pruning systems and cultivars influence the diversity of wood-colonizing fungi. *Fungal Ecology* 24: 82–93 DOI: 10.1016/j.funeco.2016.09.003
- Úrbez-Torres, J. R., Leavitt, G. M., Guerrero, J. C., Guervara, J., Gubler, W. D., 2008. Identification and pathogenicity of *Lasioidiplodia theobromae* and *Diplodia seriata*, the causal agents of bot canker disease of grapevines in Mexico. *Plant Disease* 92: 519–529. DOI: 10.1094/PDIS-92-4-0519
- Úrbez-Torres J. R., 2011. The status of Botryosphaeriaceae species infecting grapevines. *Phytopathologia Mediterranea* 50: S5–S45. DOI:10.14601/Phytopathol\_Mediterr-9316
- Vaz A.T., Del Frari G., Chagas R., Ferreira A., Oliveira H., Boavida Ferreira R., 2020. Precise nondestructive location of defective woody tissue in grapevines affected by wood diseases. *Phytopathologia Mediterranea* 59(3): 441–451. DOI: 10.14601/Phyto-11110
- Vazquez-Cooz I., Mayer R.W., 2004. Occurrence and lignification of libriform fibers in normal and tension wood of red sugar maple. *Wood and Fibers Science* 36: 56–70.
- Viala P., 1926. Recherches sur les maladie de la vigne - esca. *Annales des Epiphyties*, Fasc. 1 et 2. Paris Institut des Recherches Agronomique.
- von Arx G., Kueffer C., Fonti P., 2013. Quantifying plasticity in vessel grousing – Added value from the

- image analysis tool ROXAS. *IAWA Journal* 34: 433–445. DOI: 10.1163/22941932-00000035
- Worrall J.J., Anagnost S.E., Zabel R.A., 1997. Comparison of wood decay among diverse lignicolous fungi. *Mycologia* 89(2): 199–219. DOI: 10.1080/00275514.1997.12026772
- Yadav V., Wang Z., Wie C., Amo A., Ahmed B., ... Zhang X., 2021. Phenylpropanoid pathway engineering: An emerging approach toward plant defense. *Pathogens* 9: 312. DOI: 10.3390/pathogens.9040312
- Yadeta K.A., Thomma B.P.H.J., 2013. The xylem as battleground for plant host and vascular wilt pathogens. *Frontiers in Plant Science* 4: 97. DOI:10.3389/fpls.2013.00097
- Ye Q., Jia J., Manawasinghe I.S., Li X., Zhang W., ... Yan J., 2021. *Fomitiporia punicata* and *Phaeoacremonium minimum* associated with esca complex of grapevine in China. *Phytopathology Research* 3: 11. DOI: 10.1186/s42483-021-00087-w
- Zhang Y., Carmesin C., Kaack L., Klepsch M.M., Kotowska M., ... Jansen S., 2020. High porosity with tiny pore constrictions and unbending pathways characterize the 3D structure of intervessel pit membranes in angiosperm xylem. *Plant Cell Environ.* 43(1):116–130. DOI: 10.1111/pce.13654
- Zimmermann M.H., Jeje A.A., 1981. Vessel-length distribution in stems of some American woody plants. *Canadian Journal of Botany* 59: 1882–1892. DOI: 10.1139/b81-248